Upright, Weight-Bearing, Dynamic-Kinetic MRI of the Spine
*p*MRI/*k*MRI

J.R. JINKINS, J.S. DWORKIN*, C.A. GREEN*, J.F. GREENHALGH*, M. GIANNI*, M. GELBIEN*, R.B. WOLF*, J. DAMADIAN*, R.V. DAMADIAN*

Medical College of Pennsylvania-Hahnemann, Drexel University, Philadelphia, Pennsylvania;
** Fonar Corporation, Melville, New York*

Key words: magnetic resonance imaging spine, kinetic spine imaging, upright spine imaging, dynamic spine imaging

SUMMARY - The purpose of this study was to demonstrate the general utility of the first dedicated magnetic resonance imaging (MRI) unit enabling upright, weight-bearing *p*ositional evaluation of the spinal column (*p*MRI) during various dynamic-*k*inetic maneuvers (*k*MRI) in patients with degenerative conditions of the spine.

This study consisted of a prospective analysis of cervical and lumbar imaging examinations. All studies were performed on a recently introduced whole body MRI system (Stand-Up™ MRI, Fonar Corp, Melville, NY). The system operates at 0.6T using an electromagnet with a horizontal field, transverse to the longitudinal axis of the patient's body. Depending upon spinal level, all examinations were acquired with either a cervical or lumbar solenoidal radiofrequency receiver coil. This unit is configured with a top/front-open design, incorporating a patient-scanning table with tilt, translation and elevation functions. The unique motorized patient handling system developed for the scanner allows for vertical (upright, weight bearing) and horizontal (recumbent) positioning of all patients. The top/front-open construction also allows dynamic-kinetic flexion and extension maneuvers of the spine. Patterns of bony and soft tissue change occurring among *r*ecumbent (*r*MRI) and upright neutral *p*ositions (*p*MRI), and dynamic-*k*inetic acquisitions (*k*MRI) were sought.

Depending on the specific underlying pathologic degenerative condition, significant alterations observed on *p*MRI and *k*MRI that were either more or less pronounced than on *r*MRI included: fluctuating anterior and posterior disc herniations, hypermobile spinal instability, central spinal canal and spinal neural foramen stenosis and general sagittal spinal contour changes. No patient suffered from feelings of claustrophobia that resulted in termination of the examination.

In conclusion, the potential relative beneficial aspects of upright, weight-bearing (*p*MRI), dynamic-kinetic (*k*MRI) spinal imaging on this system over that of recumbent MRI (*r*MRI) include: the revelation of occult disease dependent on true axial loading, the unmasking of kinetic-dependent disease, and the ability to scan the patient in the position of clinically relevant signs and symptoms. This imaging unit also demonstrated low claustrophobic potential and yielded relatively high-resolution images with little motion/chemical-shift artifact.

Ricevuto il 30.07.2002

Introduction

Magnetic resonance imaging (MRI) using commercial systems has until the present been limited to acquiring scans with patients in the recumbent position. It is a logical observation that the human condition is subject to the effects of gravity in positions other than that of recumbency [1]. In addition, it is clear that patients experience signs and symptoms in dynamic maneuvers of the spinal column other than the recumbent one. For this reason, a new fully open MRI unit was configured to allow upright, partially upright, as well as recumbent imaging. This would at the same time enable partial or full weight bearing and simultaneous kinetic maneuvers of the patient's whole body or any body part. The objective was to facilitate imaging of the body in any position of normal stress, across the limits of range of motion, and importantly in the specific position of the patient's clinical syndrome. Under optimized conditions it was hoped that a specific imaging abnormality might be linked with the specific position or kinetic maneuver that reproduced the clinical syndrome. In this way imaging findings could potentially be tied meaningfully to patient signs and symptoms. Furthermore, it was anticipated that radiologically occult but possibly clinically relevant weight bearing and/or kinetic dependent disease not visible on the recumbent examination would be unmasked by the positional-dynamic imaging technique [2].

Material and Methods

This study consisted of a prospective analysis of cervical and lumbar MRI examinations. All examinations were performed on a recently introduced full body MRI system (Stand-Up ™ MRI, Fonar Corporation, Melville, NY) (figure 1). The system operates at 0.6T using an electromagnet with a horizontal field, transverse to the longitudinal axis of the patient's body.

Table 1 **Patient Positioning related variations of MRI**

• *R*ecumbent MRI: *r*MRI: Supine, recumbent imaging
• *P*ositional MRI: *p*MRI: Imaging in varying angular positions of longitudinal axis of body
• *K*inetic MRI: *k*MRI: Imaging during dynamic-kinetic somatic maneuvers (flexion, extension, rotation, lateral bending)

Depending upon spinal level, all examinations were acquired with either a cervical or lumbar solenoidal radiofrequency receiver coil. This MRI unit is configured with a top/front-open design, incorporating a patient-scanning table with tilt, translation and elevation functions. The unique MRI-compatible, motorized patient handling system developed for the scanner allows vertical (upright, weight bearing) and horizontal (recumbent) positioning of all patients. The top/front-open construction also allows dynamic-kinetic flexion and extension maneuvers of the spine.

Sagittal lumbar/cervical T1- (TR: 680, TE: 17, NEX: 3, ETL: 3) weighted fast spin echo imaging (T1FSEWI), sagittal lumbar/cervical T2- (4000, 140-160, 2, 13-15) weighted fast spin echo imaging (T2FSEWI), axial lumbar T1WI (600, 20, 2) or T1FSEWI (800, 17, 3, 3), axial cervical gradient recalled echo T2*-weighted (620-730, 22, 2) (T2*GREWI) were performed in all cervical/lumbar studies, respectively. In all cases, recumbent neutral, upright neutral, upright flexion, and upright extension imaging was performed. The patients were seated for the upright cervical examinations and for the neutral upright lumbar acquisitions, and were placed in the standing position for the lumbar kinetic studies.

Patterns of bony and soft tissue change occurring among *r*ecumbent neutral (*r*MRI) and upright neutral *p*ositions (*p*MRI), and dynamic-*k*inetic acquisitions (*k*MRI: upright flexion-extension) were sought (table 1). Specifically, degenerative spinal disease including focal intervertebral disc herniations, spinal stenosis involving the central spinal canal and spinal neural foramina, and hypermobile spinal instability were compared to other visibly normal segmental spinal levels among the rMRI, the pMRI and kMRI acquisitions (tables 2-7).

Focal disc herniations were defined as localized protrusions of intervertebral disc material that encompassed less that 25% of the total disc periphery in the axial plane; central spinal stenosis was defined as generalized narrowing of the central spinal canal in the axial and/or sagittal plane relative to that of other spinal levels; spinal neural foramen narrowing was defined as general narrowing of the neural foramina as determined from sagittal acquisitions relative to that of other segmental spinal levels; and hypermobile spinal instability was defined as relative mobility between adjacent spinal segments as compared to other spinal levels that in turn demonstrated virtually no intersegmental motion. Generally speaking, degenerative disc disease was defined as both intrinsic discal MRI signal loss as well as morphological alteration to include a reduction in superoinferior dimensional disc space height.

Alterations in sagittal spinal curvature were also noted between the neutral rMRI and pMRI acquisitions (table 8). Finally, notation was made as to whether or not the patient was referred in part because of an inability to undergo a prior MRI due to subjective feelings of claustrophobia attempted in a "closed" MRI unit.

Results

The neutral upright imaging studies (neutral-pMRI) demonstrated the assumption by the patient of the true postural sagittal lumbar cervical or lumbar lordotic spinal curvature existing in the patient at the time of the MRI examination, a feature that was partially or completely lost on the neutral recumbent examination (rMRI) (figures 2,3). In other words, this relative postural sagittal spinal curvature correction phenomenon was manifested by a change from a straight or even reversed lordotic curvature on rMRI to a more lordotic one on pMRI. Increasing severity of focal posterior disc herniation on the neutral-pMRI compared to the rMRI was noted (figure 3), and was yet worse in degree on extension-kMRI (figure 2); these posterior disc herniations were less severe on flexion-kMRI maneuvers as compared to all other acquisitions (figure 4). Absolute *de novo* appearance of disc herniation on neutral-pMRI was identified on extension-kMRI acquisitions in some cases as compared to rMRI (figure 2). A reduction of intervertebral disc height was typically noted at levels of disc degeneration (fig-

Table 2 **Dynamic spinal alterations**

• Bony Structures:	- Intersegmental Relationships - Range of Motion - Spinal Contour
• Intervertebral Discs:	- Disc Height - Disc Margin
• Ligaments:	- Ligamentotactic Effects - Ligamentopathic Effects
• Perispinal Muscles	
• Neural Tissue:	- Spinal Cord - Spinal Nerve Roots (ventral and dorsal) - Cauda Equina

Table 3 "**Telescoping" of spinal column in degenerative disease**

• Intersegmental settling: - Disc collapse - Posterior spinal facet (zygapophyseal) joint subluxation
• Annulus fibrosus redundancy
• Ligamentous redundancy
• Meningeal redundancy
• Neural redundancy

Table 4 **Types of intersegmental spinal motion**

• Eumobility: normal motion
• Hypermobility: increased motion in the X, Y, Z planes
• Hypomobility: decreased motion

Table 5 **Positional fluctuation in spinal ligaments and discs (p/kMRI)**

Ligamentotactic effects
- Intact spinal ligamentous structures
- Contained bulging peripheral disc material
- Inclusion of disc material within disc space when ligaments are tensed
- Further protrusion of disc material into perispinal space when ligaments are relaxed

Table 6 **Dysfunctional intersegmental motion (DIM)**

• DIM is a form of intersegmental hypermobility
• DIM engenders generalized accelerated intersegmental degeneration
• Mechanism of accelerated spinal degeneration: chronic, repetitive autotrauma

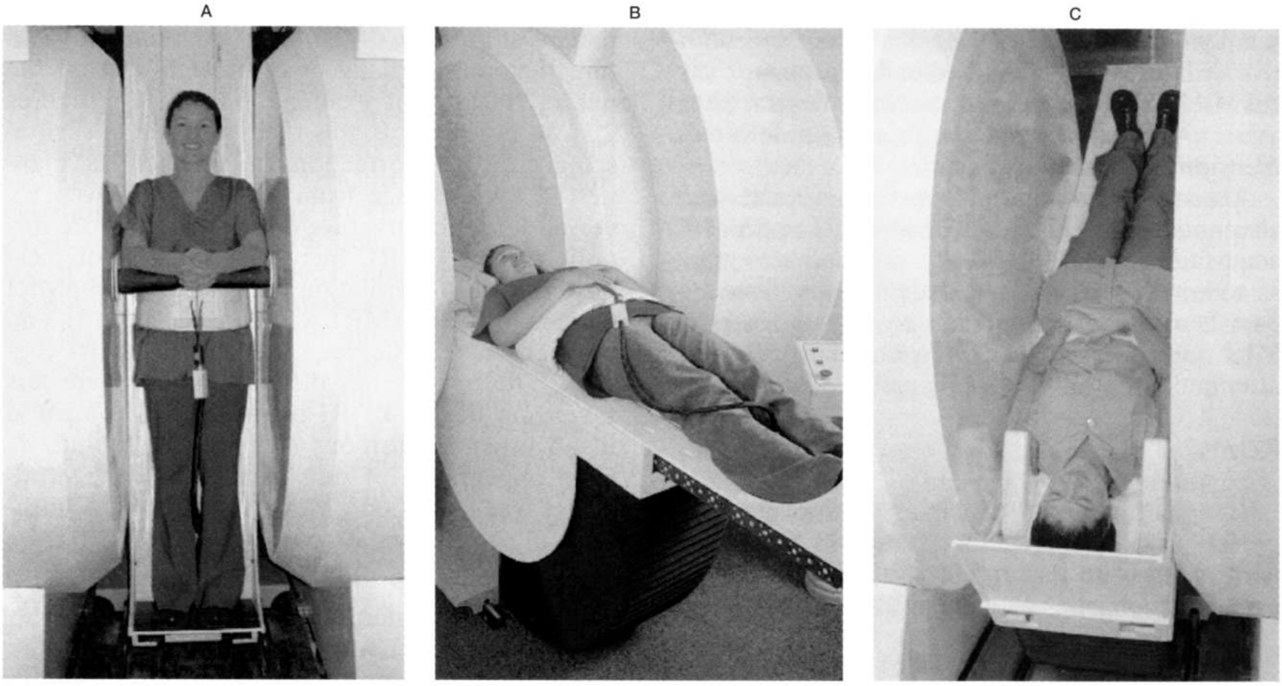

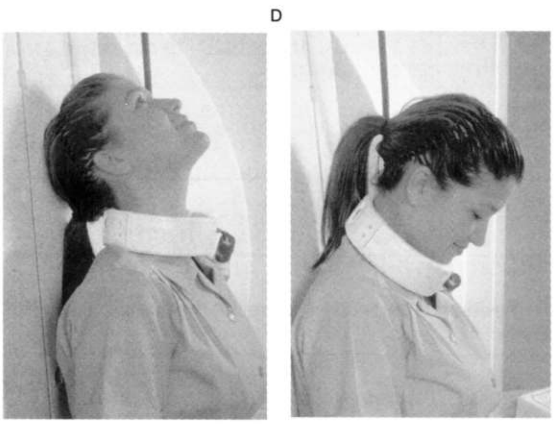

Figure 1 Various patient/table configurations of the "Stand-Up™" MRI unit: A) Patient in standing position (standing-neutral pMRI); B) patient in recumbent position (rMRI); C) patient in Trendelenberg position (negative angled pMRI); D) patient in cervical flexion-extension maneuvers (kMRI); E) patient in lumbar flexion-extension maneuvers (kMRI); F) patient in seated-upright position (seated-neutral pMRI).

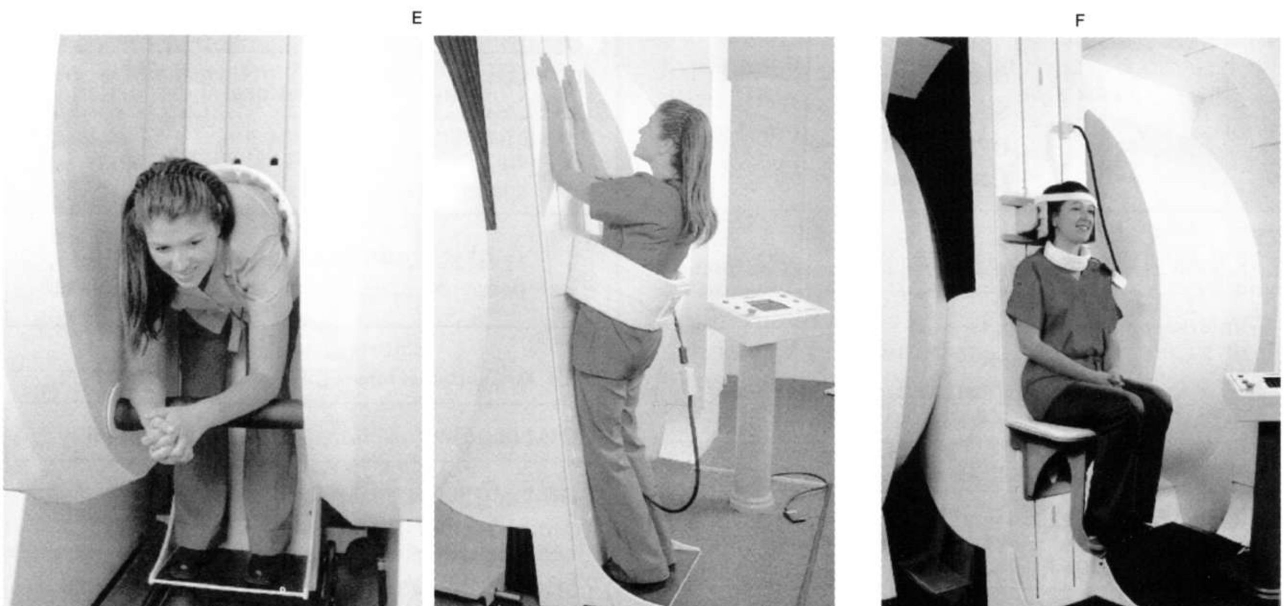

Figure 2 Sagittal cervical spinal curvature correction; unmasking of central spinal stenosis; occult herniated intervertebral disc (all images in same patient): A) recumbent midline sagittal T2-weighted fast spin echo MRI (rMRI) shows straightening and partial reversal of the sagittal spinal curvature of the cervical spine (double headed arrow). Minor posterior disc bulges/protrusions are present at multiple levels, but the spinal cord (asterisk) is not compressed. B) Upright-neutral midline sagittal T2-weighted fast spin echo MRI (pMRI) shows partial restoration of the true sagittal postural cervical curvature upon neutral-upright positioning (curved line). Note the relative increase in the posterior disc protrusion at the C5-6 level (arrowhead) and encroachment on the spinal cord (asterisk) as compared to the recumbent image (A). C) Recumbent axial T2*-weighted gradient recalled echo MRI (rMRI) through the C4-5 level shows patent neural foramina bilaterally (single headed arrows), and mild stenosis of the central spinal canal (double headed arrow). C) Upright-neutral axial T2*-weighted gradient recalled echo MRI (pMRI) through the C4-5 level shows bilateral narrowing of the neural foramina (single headed arrows). Note also the narrowing of the central spinal canal (double-headed arrows) relative to the recumbent study (D), and the compression of the underlying spinal cord [i.e., relative anteroposterior flattening of the spinal cord as compared to the recumbent image (D)].

E

F

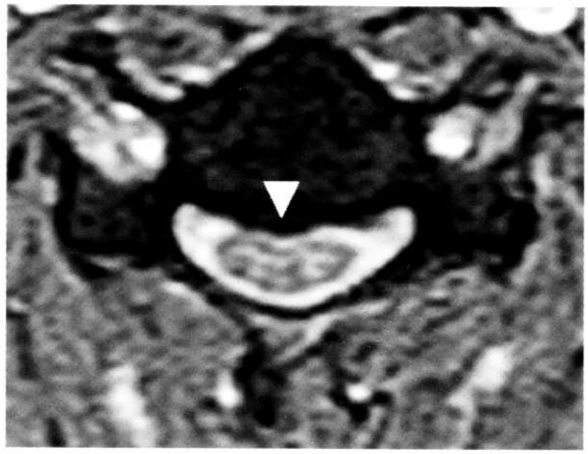

G

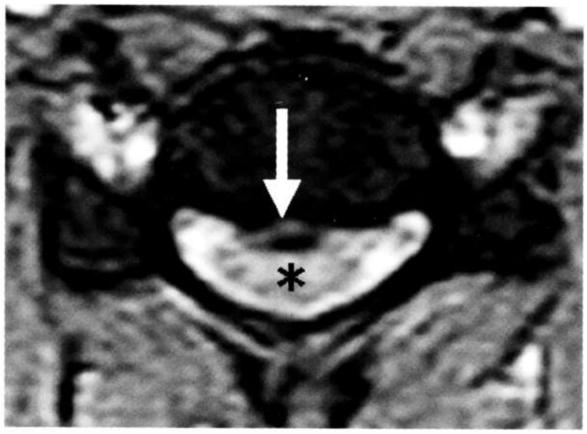

Figure 2 E) Upright-extension midline sagittal T2-weighted fast spin echo MRI (extension kMRI) shows further posterior protrusion of the intervertebral discs at multiple levels (arrows) and anterior infolding of the posterior spinal ligaments (arrowheads), resulting in overall worsening of the stenosis of the central spinal canal. Note the impingement (i.e., compression) of the underlying spinal cord (asterisk) by these encroaching spinal soft tissue elements. F) Recumbent axial T2*-weighted gradient recalled echo MRI (rMRI) at the C5-C6 disc level shows posterior paradiscal osteophye formation (arrowhead) extending into the anterior aspect of the central spinal canal. Note that the cervical spinal cord is atrophic, but there is a rim of CSF hyperintensity entirely surrounding the cord. G) Upright-extension axial T2*-weighted gradient recalled echo MRI (extension kMRI) revealing (extension-related) focal posterior disc herniation (arrow). Note the overall increased stenosis of the central spinal canal and the compression-indentation of the underlying cervical spinal cord (asterisk).

ures 3,4). Increasing severity of central spinal canal stenosis was identified on neutral-pMRI and on extension-kMRI acquisitions, as compared to rMRI, and was overall most severe on extension and least severe on flexion-kMRI acquisitions (figures 2,5). Similarly, increasing severity of spinal neural foramen stenosis was identified on neutral-pMRI (figures 3), as compared to rMRI, and was overall most severe on extension and least severe on flexion-kMRI acquisitions (figure 6). Increasing central spinal canal narrowing with spinal cord compression on extension-kMRI was identified in some cervical examinations (figure 2) as compared to recumbent rMRI, neutral-pMRI and flexion-kMRI maneuvers. Translational sagittal plane intersegmental hypermobility was identified at some levels associated with degenerative disk disease and minor anterolisthesis of a degenerative nature (figures 5,7). Postoperative spinal stability was identified across levels of prior surgical fusion (figure 8). No examination was uninterpretable based on patient motion during any portion of the MRI acquisitions. No patient was unable to complete the entire examination due to subjective feelings of claustrophobia.

Discussion

Conventional recumbent MRI, or *r*MRI, is obviously inadequate theoretically for a complete and thorough evaluation of the spinal column and its contents. The biomechanics of human condition includes both weight bearing body positioning, or *p*MRI, as well as complex kinetic maneuvers, or *k*MRI in three dimensions [3-6]. The present MRI unit was intended to address these considerations.

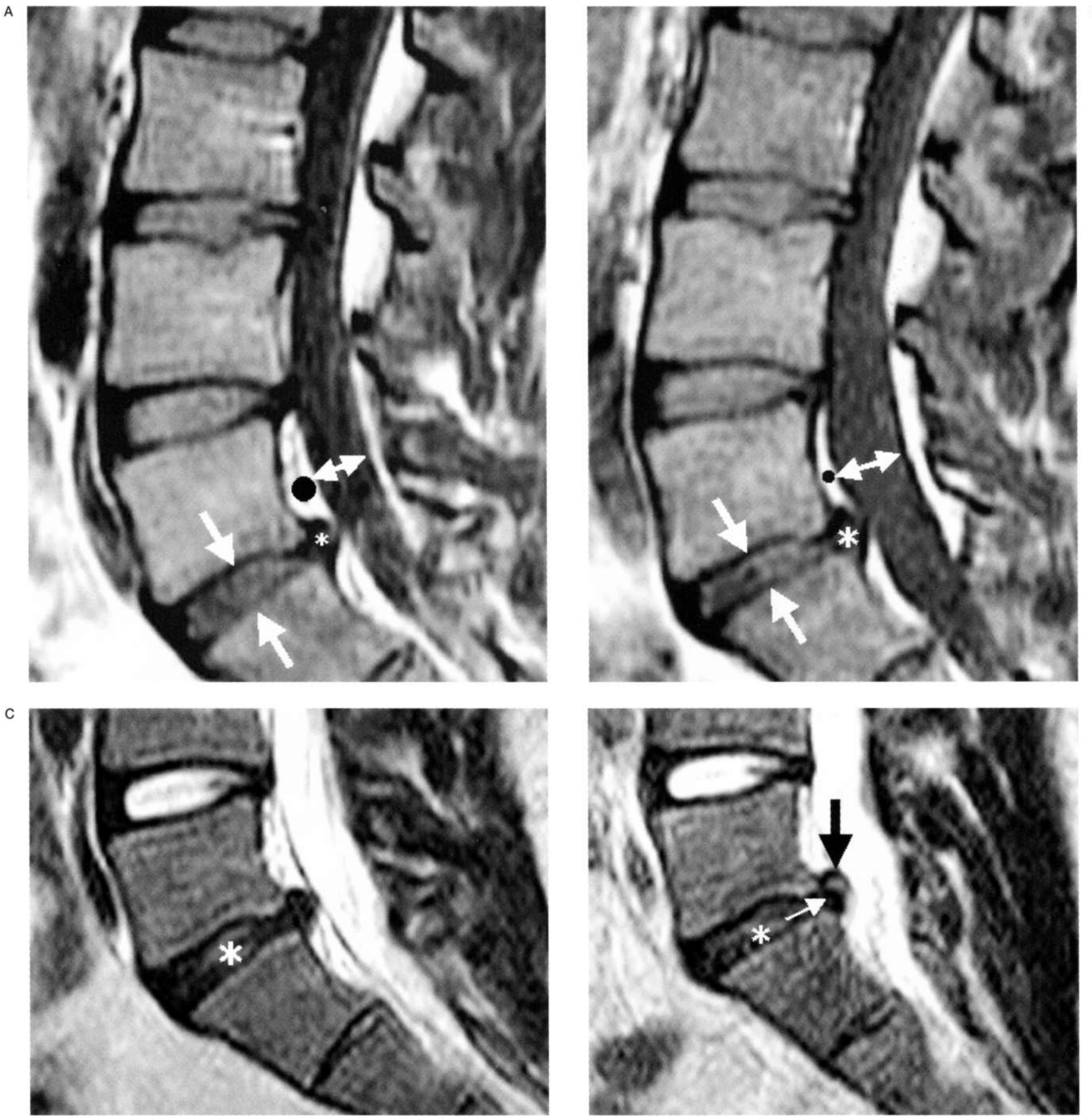

Figure 3 Effects of gravity on the intervertebral disc, thecal sac, and spinal neural foramina; true sagittal postural lumbosacral curvature: A) Recumbent midline sagittal T1-weighted fast spin echo MRI (rMRI) shows a focal disc herniation at L5-S1 (asterisk) and mild narrowing of the superoinferior disc height at this level (single headed arrows). Note also the anteroposterior dimension of the thecal sac (double headed arrow), and the size of the anterior epidural space (dot) at the L4 level. B) Upright-neutral (standing) midline sagittal T1-weighted fast spin echo MRI (pMRI) shows minor further narrowing of the height of the L5-S1 intervertebral disc (single headed arrows) and enlargement of the posterior protrusion of the disc herniation at this level (asterisk) (compare with A). Also note the generalized expansion of the thecal sac (double headed arrow) because of gravity-related hydrostatic CSF pressure increases, and the consonant decrease in the dimensions of the anterior epidural space (dot: theoretically caused by a reduction in volume of the anterior epidural venous plexus). Finally, note that the upright-standing spine now assumes the true sagittal postural curvature on this image, as compared to the recumbent image (compare with A). C) Recumbent midline sagittal T2-weighted fast spin echo MRI (rMRI) shows the posterior disc herniation at L5-S1 (asterisk). D) Upright-neutral midline sagittal T2-weighted fast spin echo MRI (pMRI) shows further narrowing of the L5-S1 intervertebral disc (asterisk: compare with C) and a new component to the posterior disc herniation (black arrow) resulting in overall enlargement of the size of the herniation (compare with C). Apparently, this observed enlargement is caused by intradiscal fluid (i.e., water) and/or disc material exiting via an unvisualized posterior radial annular tear (white arrow) into the epidural space. Because fluids and semifluids (water; nucleus pulposis) are noncompressible, the reduction in size of the disc volume makes it necessary that the intradiscal fluids-semifluids evacuate via some route, a radial annular tear being the most likely pathway. Some degree of radial peripheral disc bulging may also contribute to this phenomenon.

E

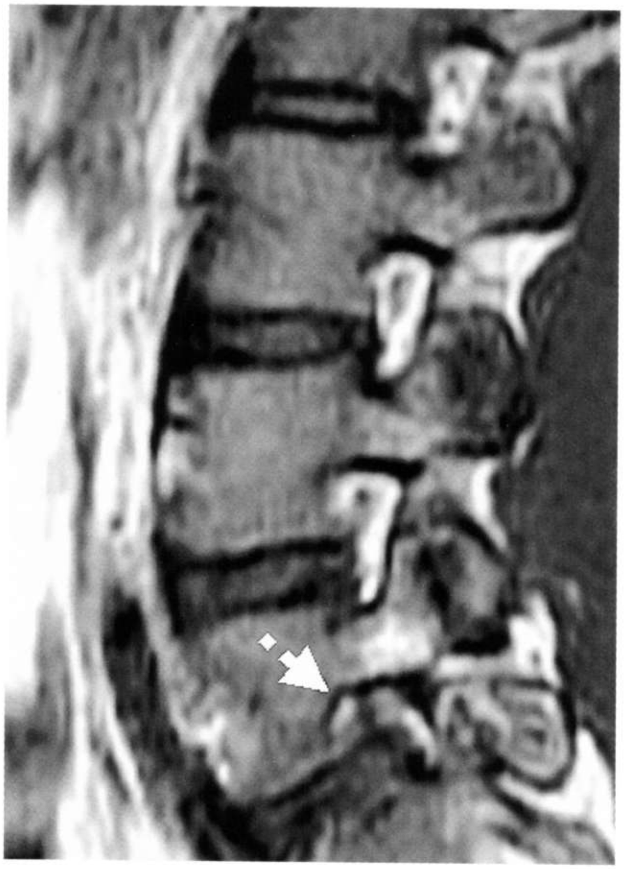

F

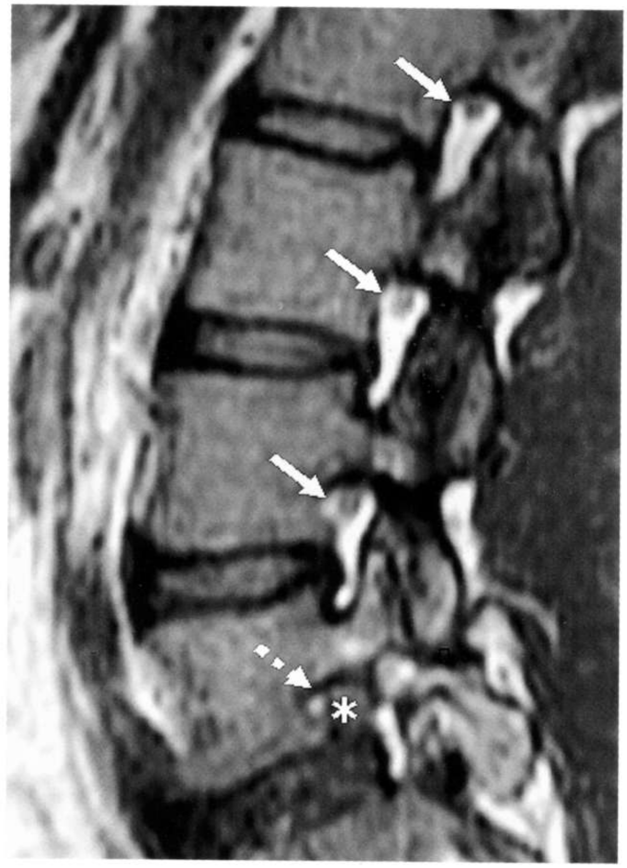

Figure 3 E) Recumbent midline parasagittal T1-weighted fast spin echo MRI (rMRI) on the patient's left side shows narrowing of the L5/S1 spinal neural foramen (dashed arrow) as a result of posterior disc protrusion, intervertebral disc space narrowing and paradiscal osteophyte formation. F) Upright-neutral midline parasagittal T1-weighted fast spin echo MRI (pMRI) on the patient's left side reveals minor generalized narrowing of all of the spinal neural foramina (solid arrows), including the L5/S1 level (dashed arrow) (compare with recumbent examination, E). At some point in this stenotic process, the exiting neurovascular bundle (asterisk) will undergo compression and may become symptomatic.

Both occult weight bearing disease (e.g., focal intervertebral disc herniations, spinal stenosis, thecal sac volumetric change), and kinetic dependent disease (e.g., disc herniations, spinal stenosis, hypermobile instability) of a degenerative nature [7-23] were unmasked by the p/kMRI technique. In addition, a true assessment of the patient's sagittal postural spinal lordotic curvature was possible on neutral upright pMRI, thereby enabling better evaluation of whether the loss of curvature was due to patient positioning (i.e., rMRI) or as a probable result of somatic perispinal muscular guarding or spasm (figures 2,3). Axial loading and dynamic flexion-extension studies by other researchers have borne these varied observations out [24-38].

Simple upright or upright pMRI, showed a phenomenon here termed "telescoping" whereby the levels of generalized intersegmental spinal degeneration showed a collapse of the spine into itself (figure 4) [39].

Consequent redundancy of the discal, ligamentous and meningeal tissues of the spine resulted in increased degrees of central canal and lateral recess spinal stenosis, while craniocaudal shortening of the spine associated with telescoping caused increased degrees of neural foramen stenosis (figure 3). On occasion, the degree of frank posterior disc herniation was seen to enlarge with upright pMRI (figure 3). This latter finding would seem to be an important observation, obviously improving the qualitative nature of the analysis in relevant cases of disc herniation. Finally, upright-neutral imaging frequently showed increasing degrees of sagittal plane anterolisthesis, both in degenerative spondylolisthesis and in some cases of spondylolytic spondylolisthesis [40].

Upright extension kMRI tended to show greater degrees of central canal and neural foramen stenosis, while flexion kMRI revealed a lessening or complete resolution of the same central canal and neural foramen narrowing (figures 5,6). These phenomena were only observed at levels of disc degeneration (i.e., both disc desiccation and disc space narrowing) [41,42]. In exceptional cases, *de*

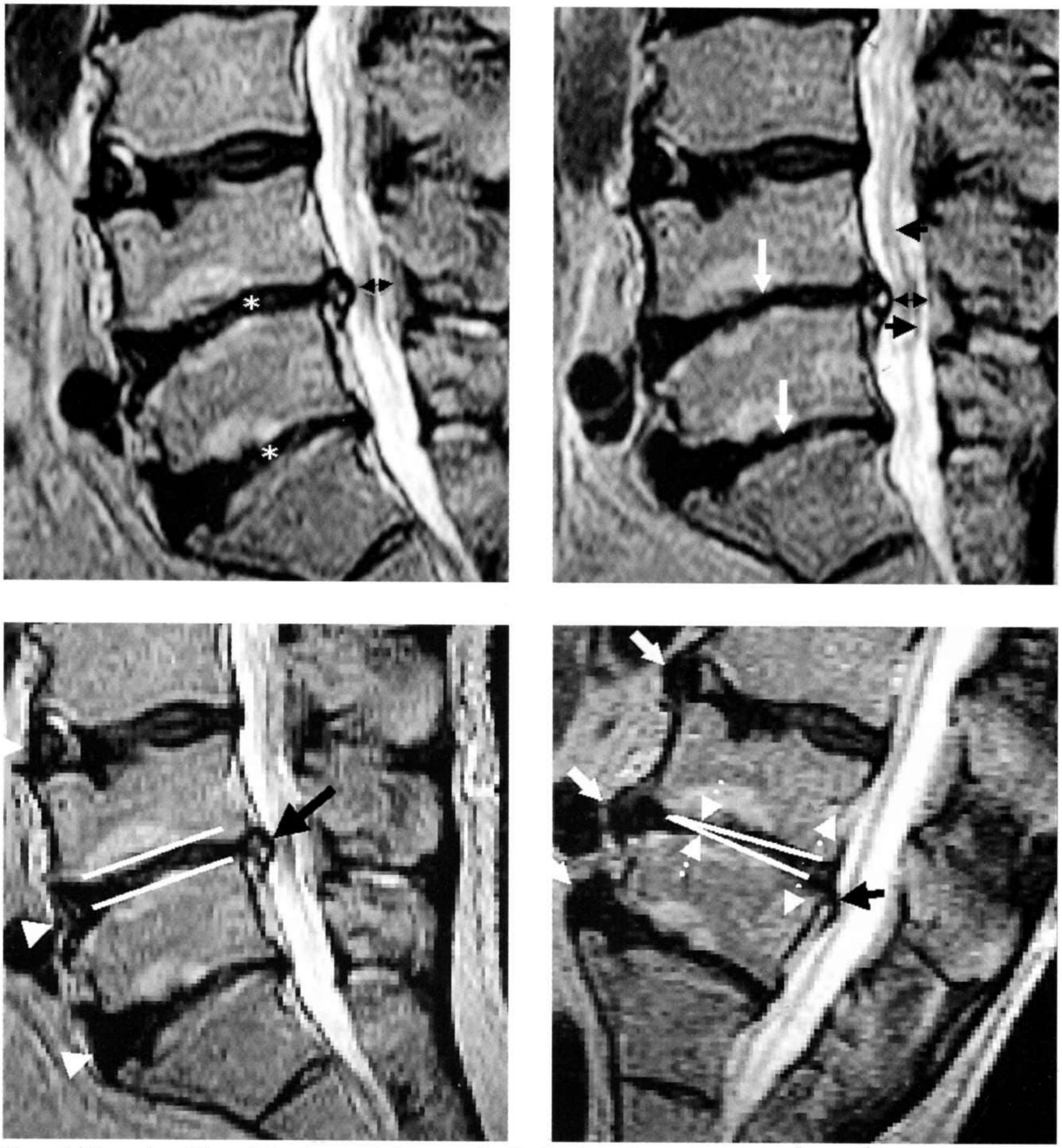

Figure 4 Telescoping of the spinal column; reducing posterior disc herniation; increasing anterior disc protrusions; dysfunctional intersegmental motion. A) Recumbent midline sagittal T2-weighted fast spin echo MRI (rMRI) showing degenerative disc disease at all levels, especially severe at L4-L5 and the L5-S1 levels (asterisks). A focal posterior disc herniation is noted at the L4-L5 level. Note the narrowed (i.e., stenotic) anteroposterior dimension of the thecal sac at the L4-L5 level (double headed arrow). B) Upright-neutral midline sagittal T2-weighted fast spin echo MRI (pMRI) revealing further gravity-related narrowing of the intervertebral discs at multiple levels (white arrows), as compared to the upright-neutral examination (rMRI: A). This represents telescoping of the spinal column. Note also the minor increase in narrowing of the anteroposterior dimension of the thecal sac (double headed arrow), and the increased redundancy of the nerve roots of the cauda equina (black arrows). C) Recumbent midline sagittal T2-weighted MRI showing the relative parallel surfaces of the vertebral end plates at L4-L5 (white lines), and the flat surfaces of the anterior aspects of the intervertebral discs at multiple levels (arrowheads). Note again the posterior disc herniation at the L4-5L level (arrow). D) Upright-flexion midline T2-weighted fast spin echo MRI (kMRI) showing increases in size of the anterior disc protrusions at multiple levels (white solid arrows) and a reduction of the posterior disc herniation at the L4-L5 level (black arrow), as compared to the r/pMRI studies. Also note the opening up (i.e., enlargement) of the posterior aspect and the closing (i.e., narrowing) of the anterior aspect of the L4-L5 disc space (dashed white arrows), with resulting anterior angulation of the vertebral end plates (white lines). The latter phenomenon represents dysfunctional intersegmental motion. Finally, note the hypersplaying of the spinous processes [hyperexpansion of the interspinous space(s)], indicating rupture of the interspinous ligament(s).

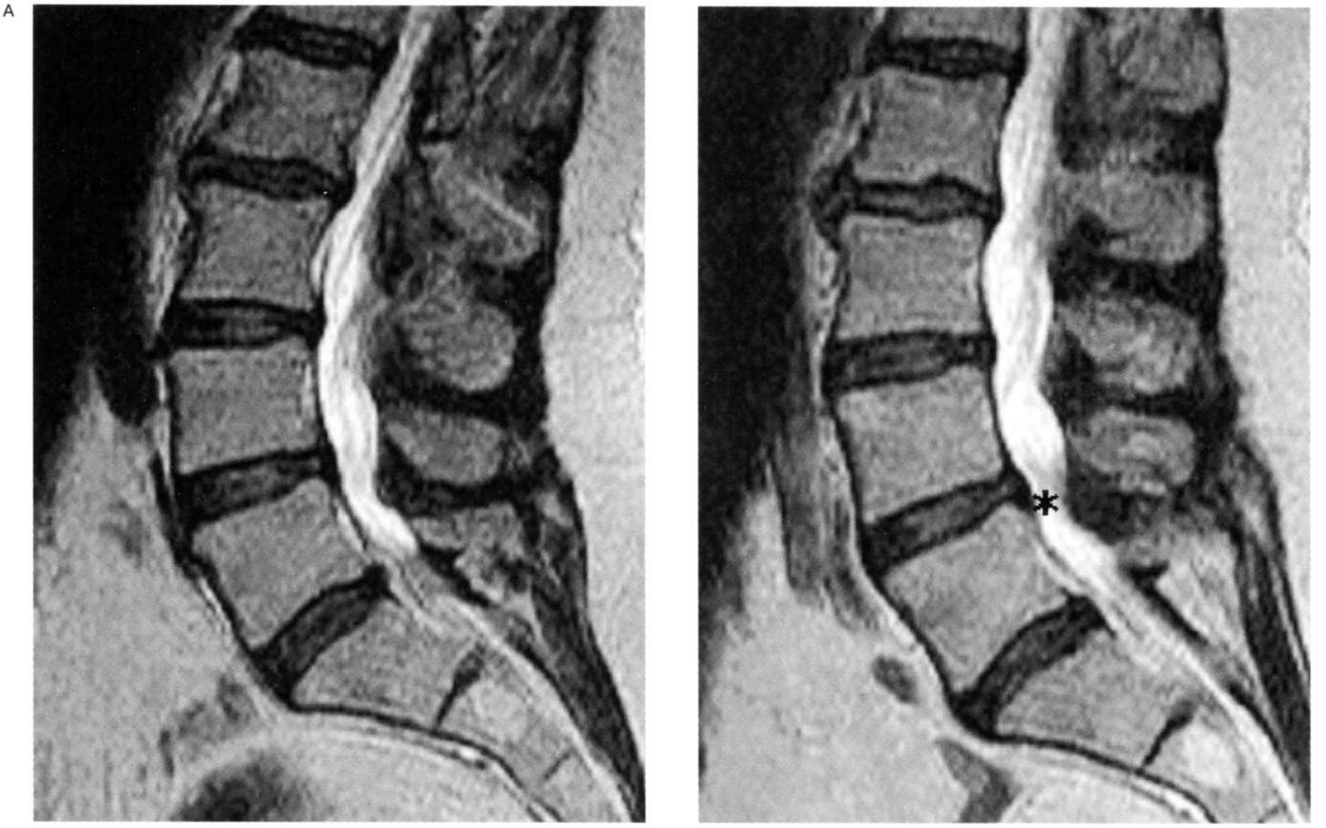

Figure 5 Worsening-reducing central spinal canal stenosis on dynamic-kinetic MRI (kMRI); minor translational intersegmental hypermobile instability on dynamic-kinetic MRI (kMRI). A) Recumbent midline sagittal T2-weighted fast spin echo MRI (rMRI) shows mild, generalized spondylosis and minor generalized narrowing of the central spinal canal. B) Upright-neutral midline sagittal T2-weighted fast spin echo MRI (pMRI) shows very minor worsening of the central spinal canal stenosis inferiorly (*) relative to the recumbent image (A). Note the assumption by the patient of the true postural sagittal lordotic curvature of the lumbosacral spine as compared to the recumbent examination.

novo posterior disc herniations were revealed only on upright-extension kMRI (figure 2). When present in the cervical spine, such cases invariably showed compression of the underlying spinal cord. Overall, this was felt to be one of the most important observations noted in this study. Interestingly, some of the posterior disc herniations became less severe when upright flexion kMRI was performed (figure 4).

This would seem to be worthy of preoperative note to those surgeons that operate on the spine in positions of flexion. Presumably this phenomenon is caused by a *ligamentotactic effect:* the intact fibers of the anterior and posterior longitudinal ligaments and the intact peripheral annular fibers have effects upon the underlying disc material, alternately allowing more disc protrusion when lax, and less protrusion when taught. It was noted that all cases of fluctuating intervertebral disc herniation had MRI signal loss compatible with desiccation as well as intervertebral disc space height reduction [43,44].

These disc findings were also invariably true in cases of sagittal ("x") plane hypermobile spinal instability [45-55]. It was possible to judge even minor degrees of translational hypermobile spinal instability (e.g., mobile antero- or retrolisthesis) grossly as well as by using direct region of interest measurements (figures 5,7). The kMRI technique obviously does not suffer from the effects of magnification and patient positioning errors potentially inherent in conventional radiographic dynamic flexion-extension studies traditionally used in these circumstances. These instances of intersegmental hypermobility seem in part to be a manifestation of spinal *ligamentopathy* [56-57]. As the principal roles of spinal ligaments are to stabilize the segments of the spine and also to limit the range of motion that the spinal segments can traverse, degenerative stretching or frank rupture of these ligaments will predictably allow some degree of intersegmental hypermobility [58-63].

Other alterations in the intervertebral discs and posterior spinal facet joints will have either posi-

C

D

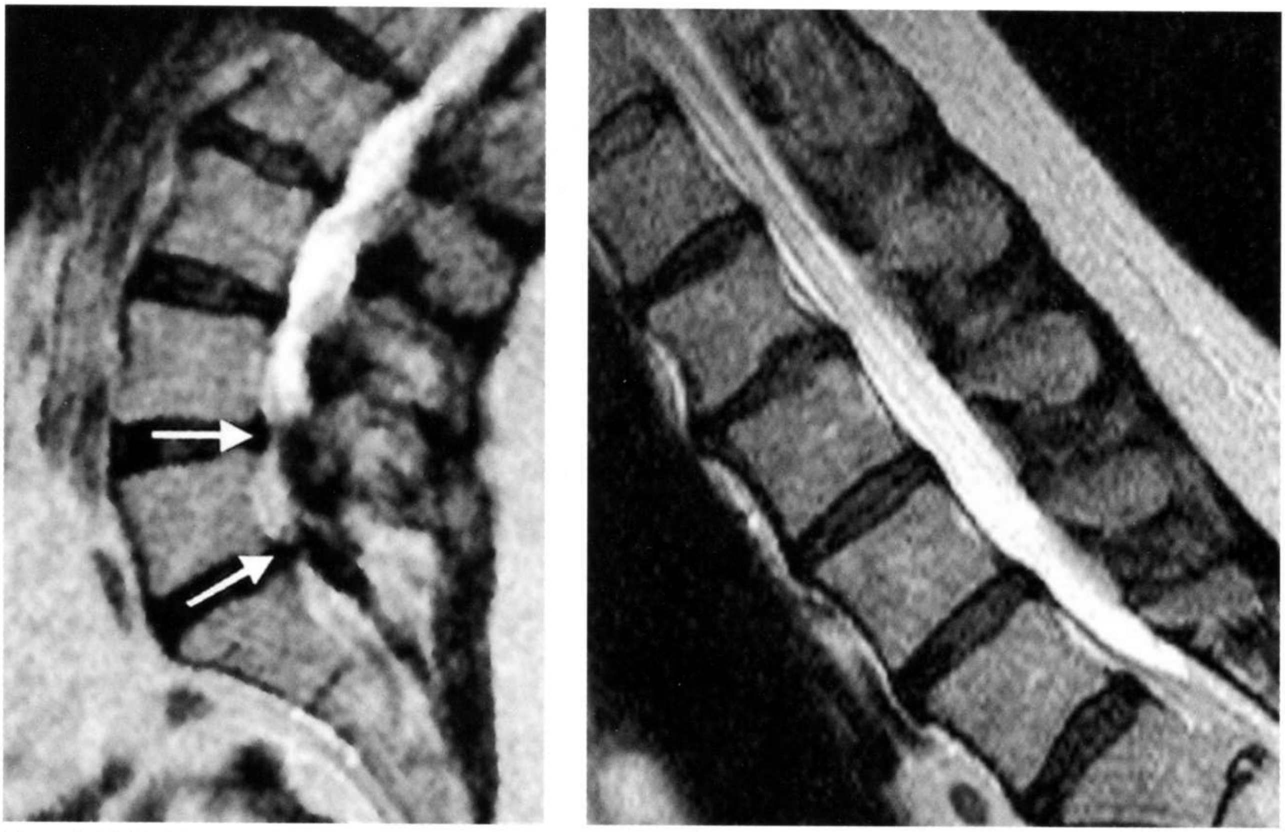

Figure 5 C) Upright-extension midline sagittal T2-weighted fast spin echo MRI (kMRI) reveals severe worsening of the central spinal canal stenosis in the lower lumbar area (arrows: L4-L5, L5-S1). This results from a combination of factors, including redundancy of the thecal sac and spinal ligaments and increasing posterior protrusions of the intervertebral discs at L4-5 and L5-S1. D) Upright-flexion midline sagittal T2-weighted fast spin echo MRI (kMRI) demonstrates complete reduction of the posterior disc protrusions at the L4-5 and L5-S1 levels, and resolution of the central spinal canal stenosis at these lumbar segments (compare with C). Also note that there is minor anterolisthesis at the L2-3 and L4-5 levels as compared to the neutral examinations (A,B), indicating associated mild translational intersegmental hypermobile instability at these levels.

tive (i.e., hypermobility) or negative (i.e., hypomobility) effects upon intersegmental motion [64-67].

Also noted at levels of disc degeneration was a sagittal plane hypermobile "rocking" of the vertebrae in relationship to each other (figures 4,6) [68]. Observation of the opposed adjacent vertebral endplates in such cases showed them to move in relationship to each other to a much greater de-

Table 7 **Translational hypermobile instability of the spinal column**

Ligamentopathic alterations: ligamentous stretching/rupture
- Mobile translational antero- and retrolisthesis (X-plane)
- Mobile latero- and rotolisthesis (Z and Y-planes)
- Dynamic overextension of spinal range(s)of motion (X, Y, Z planes)

Table 8 **Types of upright postural spinal curvature**

• Normal curvature - Cervical: lordotic - Thoracic: kyphotic - Lumbar: lordotic
• Exaggerated curvature - Hyperlordosis - Hyperkyphosis
• Loss of sagittal spinal curvature (straight spine) - Hypolordosis - Hypokyphosis
• Coronal plane scoliosis (direction of convex curve) - Leftward: levoscoliosis - Rightward: dextroscoliosis - Serpentine: serpentine scoliosis

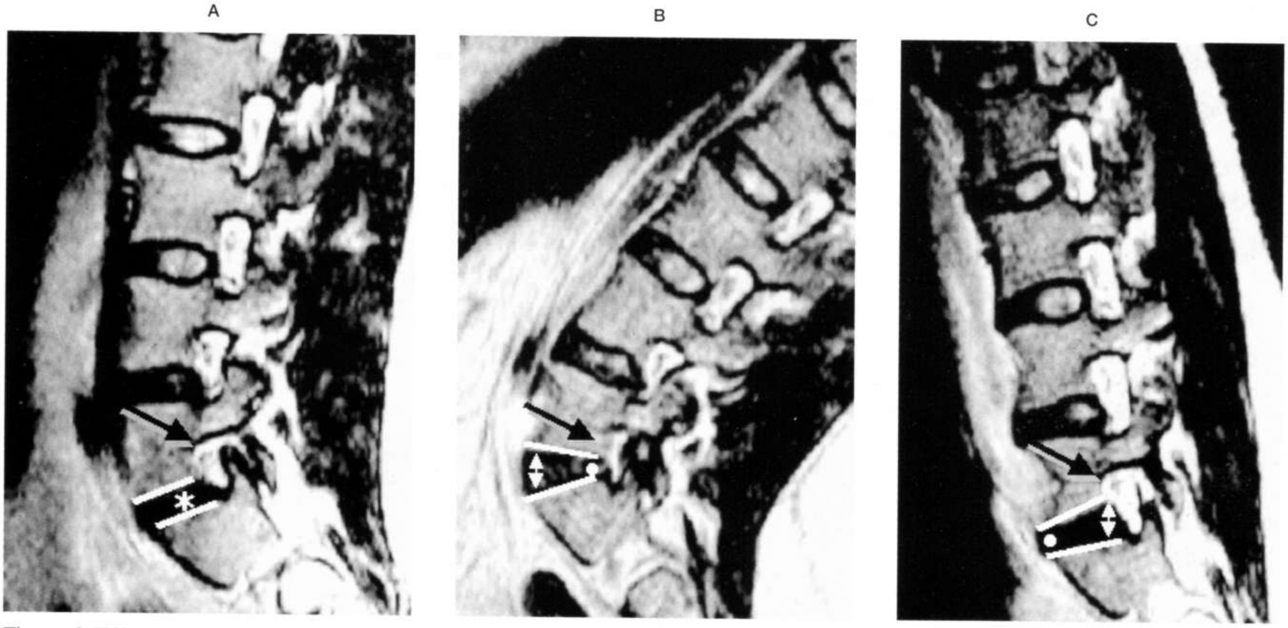

Figure 6 Effects of dynamic-kinetic maneuvers (kMRI) on spinal neural foramina at levels of degenerated disc disease and theoretical ligamentous laxity (i.e., ligamentopathy); dysfunctional intersegmental motion. A) Recumbent parasagittal T2-weighted fast spin echo MRI (rMRI) shows intervertebral disc degeneration at the L5-S1 level (asterisk). Note the mild narrowing of the neural foramen (arrow) at this level (i.e., minor foraminal stenosis), and the near parallel surfaces of the vertebral end plates (lines). B) Upright-extension parasagittal T2-weighted fast spin echo MRI (kMRI) reveals further narrowing of the neural foramen at L5-S1 (arrow) relative to the recumbent image (A). Note the opening of the anterior aspect of the disc space (double headed arrow), closing of the posterior aspect of the disc space (dot), and resulting anterior angulation of the vertebral endplates (lines). The neural foramina at other levels are minimally narrowed as compared to the recumbent image (A). C) Upright-flexion parasagittal T2-weighted fast spin echo MRI (kMRI) demonstrates opening of the neural foramen at L5-S1 (arrow), the opening of the posterior aspect of the disc space (double headed arrow), closing of the anterior aspect of the disc space (dot). Note the posterior angulation of the vertebral end plates (lines). Figures B, C illustrate dysfunctional intersegmental motion in addition to the dynamic changes in the size of the neural foramen at levels of disc degeneration and theoretical ligamentous laxity (i.e., ligamentopathy). The neural foramina at other levels are somewhat enlarged as compared to the recumbent and the extension images (A,B).

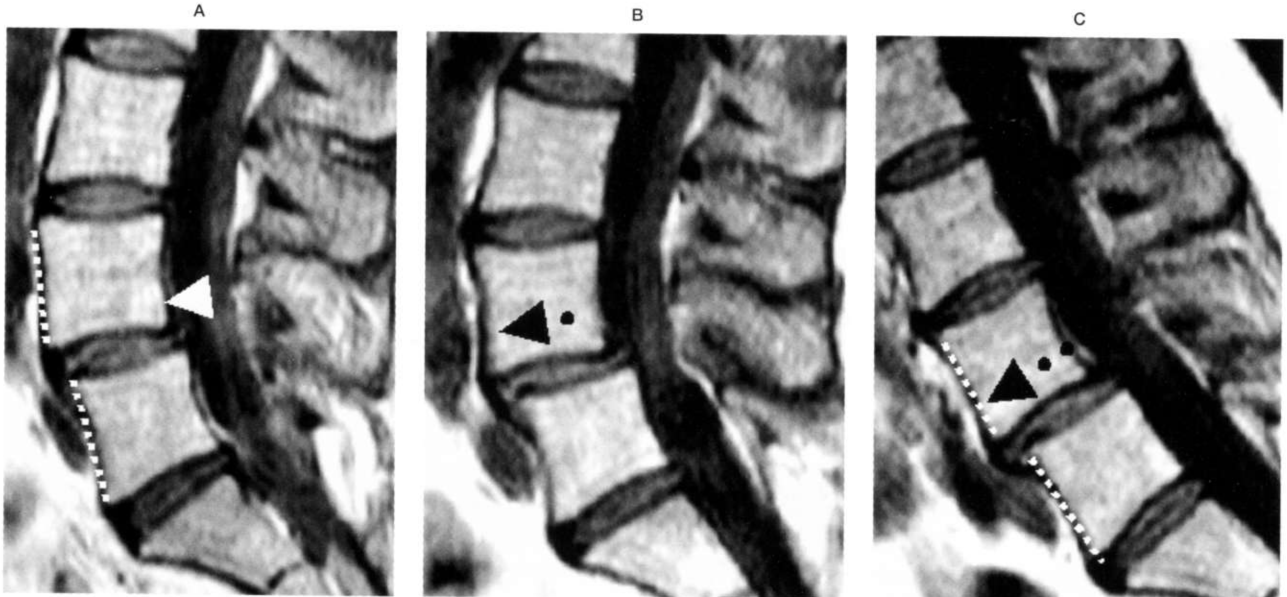

Figure 7 Translational hypermobile spinal instability associated with degenerative anterior spondylolisthesis related in part to theoretical ligamentous laxity (i.e., ligamentopathy). A) Recumbent midline sagittal T1-weighted fast spin echo MRI (rMRI) shows minor, less than grade I, anterior spondylolisthesis at the L4-5 level (arrowhead). The pars interarticularis was intact on both sides at this level. Note the relationship between the anterior surfaces of the L4 and L5 vertebral bodies (dashed lines). B) Upright-neutral midline sagittal T1-weighted fast spin echo MRI (pMRI) reveals minor worsening of the anterior slip of L4 on L5 (dashed arrow), as compared to the recumbent examination. C) Upright-flexion midline sagittal T1-weighted fast spin echo MRI (kMRI) demonstrates further anterior subluxation of L4 on L5 in flexion (dashed arrow), as compared to figures A,B. This demonstrates the dynamic translational hypermobile instability sometimes associated with degenerative spondylolisthesis and in part related to ligamentopathy. Note the relationship between the anterior surfaces of the L4 and L5 vertebral bodies (dashed lines), and the difference as compared to the recumbent image (A).

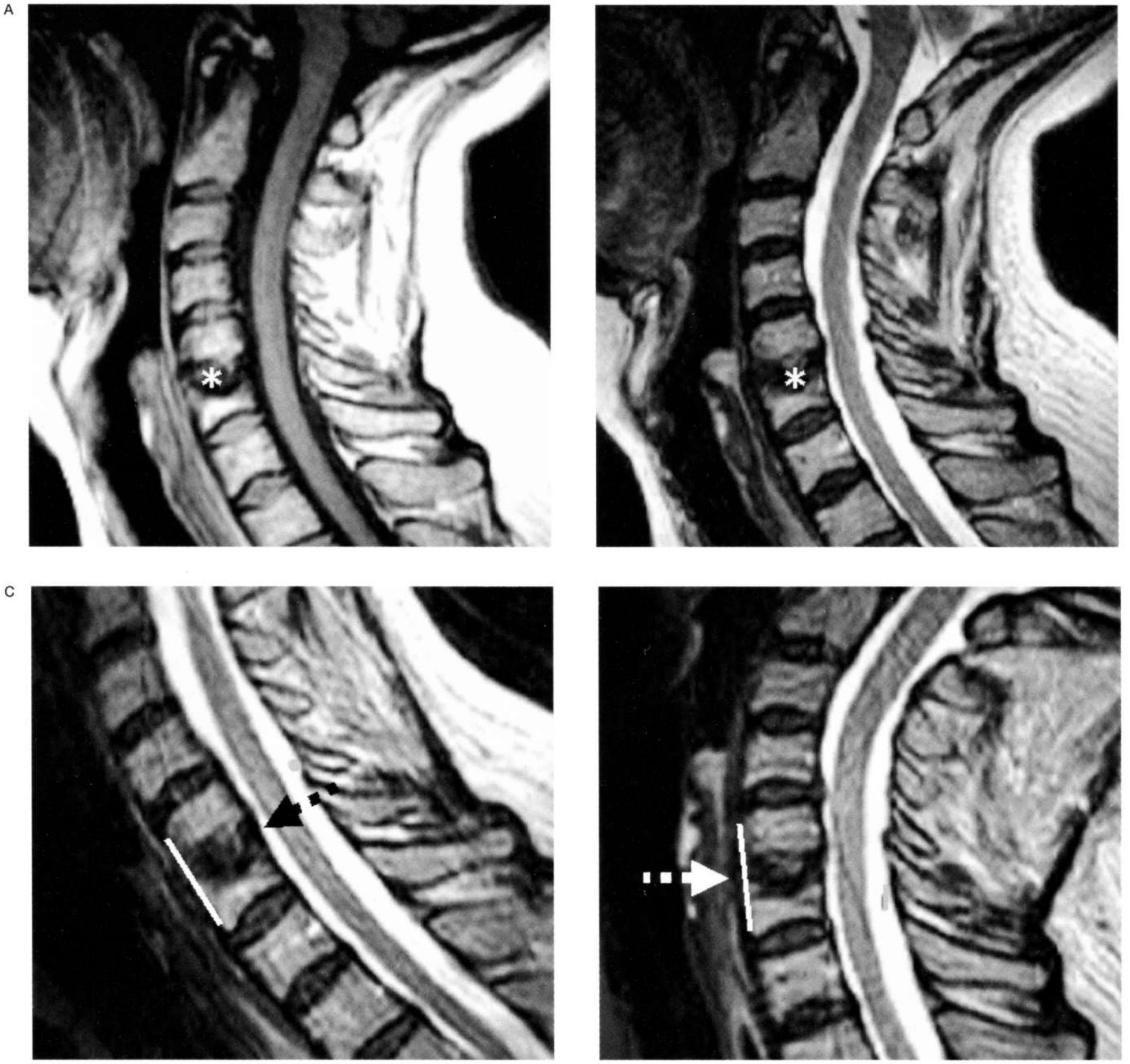

Figure 8 Postoperative intersegmental fusion stability (four years status-post clinically successful interbody bone graft fusion). A) Upright-neutral midline sagittal T1-weighted fast spin echo MRI (pMRI) shows the surgical fusion at C5-C6 (asterisk); autologous bony dowels were used for the original fusion performed 4 years prior to the current examination. Note the normal bony intersegmental vertebral alignment and normal upright postural sagittal lordotic curvature. B) Upright-neutral midline sagittal T2-weighted fast spin echo MRI (pMRI) again shows the intersegmental fusion (asterisk). Note the good spatial dimensions of the CSF surrounding the spinal cord. C) Upright-flexion (arrow) midline sagittal T2-weighted fast spin echo MRI (kMRI) shows no intersegmental slippage at, suprajacent to, or subjacent to the surgically fused level (solid line). Note the maintenance of the anteroposterior dimension of the central spinal canal. D) Upright-extension (arrow) midline sagittal T2-weighted fast spin echo MRI (kMRI) again reveals no intersegmental hypermobile instability (i.e., no intersegmental mobility: solid line) or central spinal canal compromise at any level.

gree than is observed at levels with normal intervertebral discs as judged by MRI (figures 4,6). This is here termed as *dysfunctional intersegmental motion* (DIM).

The significance of DIM is the theoretical possibility that such pathologic vertebral motion may engender generalized accelerated intersegmental degeneration due to the effects of micro-autotrauma over long periods of time. The self-protecting spinal mechanisms inherent in the normal intervertebral discs and intact spinal ligaments are lacking in such cases, perhaps initiating a progressive degenerative cascade of degenerative *autotramatizing hypermobility*.

A

B

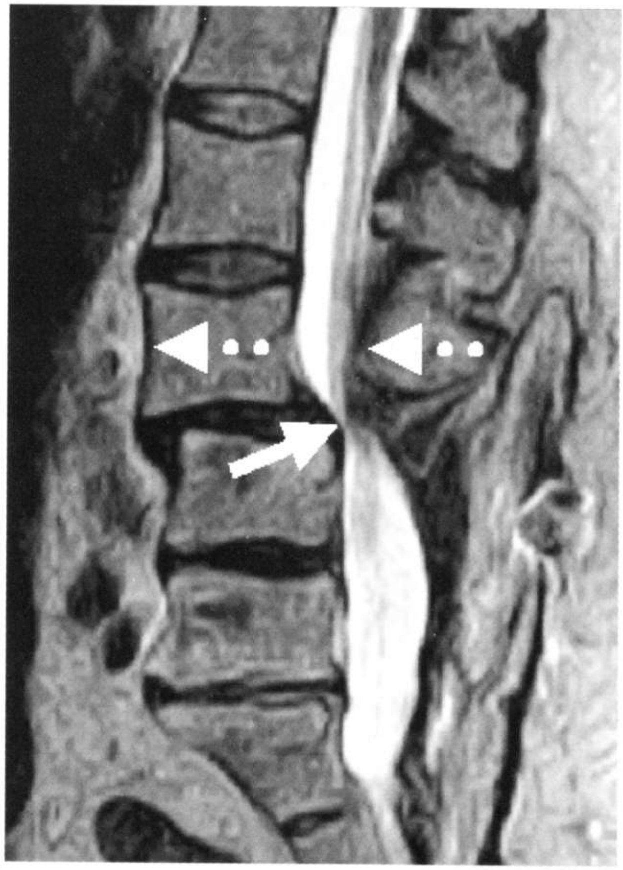

Figure 9 Postoperative intersegmental hypermobile instability at segment above fusion, 5 years following bilateral fusion (pedicle screws and rods extending between L4-S1) and bilateral laminectomy at the L4-S1 levels. A) Recumbent midline sagittal T1-weighted fast spin echo MRI (rMRI) shows bilateral laminectomy extending from L4-S1 (arrowheads). The patient also had bilateral pedicle screws and rods extending from and to the same levels (not shown). No metallic artifact is present because the surgical materials were composed of titanium. B) Sagittal-upright-sitting (i.e., partial flexion) midlineT2-weighted fast spin echo MRI (p/kMRI) demonstrates marked anterior slip of the L3 vertebral body upon the L4 vertebra (dashed arrows). Also note the resultant marked stenosis of the central spinal canal at the L3-4 level (solid arrow), and resultant encroachment of the bony structures of the spine upon the cauda equina (courtesy of M. Rose, M.D.).

Table 9 **Combined effects of spinal degeneration with telescoping, diskopathy, ligamentopathy, hypermobile instability, & DIM**

• Spinal Stenosis [central spinal canal, lateral recesses (subarticular zone), neural foramina]
• Spinal Cord/Nerve Compression
• Somatic Nerve Ending Irritation
• Neuromuscular/Ligamentous Autotrauma
• Related Patient Signs/Symptoms

Table 10 **Clinicoradiologic relevance of *p/k*MRI**

• Patient care considerations - Improvement of imaging sensitivity over that of recumbent examinations
• Medicolegal aspects - Revelation of diagnoses missed on recumbent examinations
• Worker's compensation - Revelation of occult pathology not found on recumbent examinations
• Economic factors

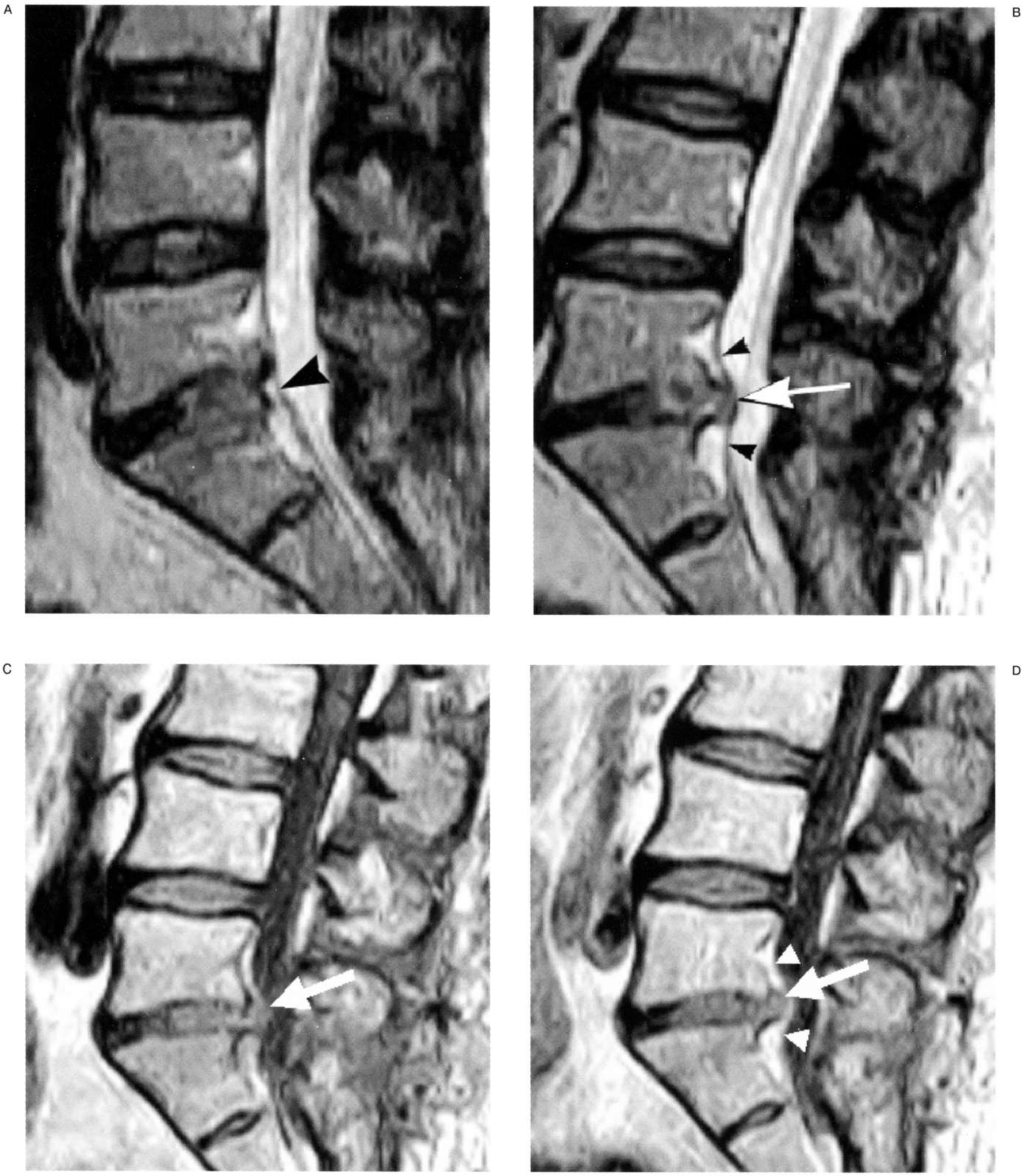

Figure 10 Postoperative fluid disc herniation eight months following partial right-sided discectomy. A) Recumbent midline sagittal T2-weighted fast spin echo MRI (rMRI) shows a flat posterior surface (arrow) of the L5-S1 intervertebral disc. B) Upright-neutral midline sagittal T2-weighted fast spin echo MRI (pMRI) reveals a focal posterior disc herniation extending from the L5-S1 intervertebral disc space. Note the tenting of the posterior longitudinal ligament and the thecal sac (arrowheads) secondary to the mass effect of the epidural disc herniation. C) Upright-neutral midline sagittal T1-weighted fast spin echo MRI (pMRI) shows a poorly defined mass (arrow) extending posteriorly from the L5-S1 disc space. D) Upright-neutral midline sagittal T1-weighted fast spin echo MRI (pMRI) following the IV administration of gadolinium demonstrates peripheral rim enhancement surrounding the centrally nonenhancing disc herniation (arrow). Also again note the tenting of the posterior longitudinal ligament and dura mater (arrowheads) secondary to the mass effect of the epidural disc herniation (courtesy of M. Rose, M.D.).

A B

Figure 11 Lateral bending maneuver (example: normal case). A) Standing-lateral bending coronal T1-weighted fast spin echo MRI (kMRI) shows multilevel disc degeneration, but normal right lateral bending of the spinal column in this volunteer. There is no evidence of lateral translational dysfunctional intersegmental motion. B) Standing-lateral bending coronal T2-weighted fast spin echo MRI (kMRI) again shows the normal right lateral bending appearance of the spinal column.

A B C

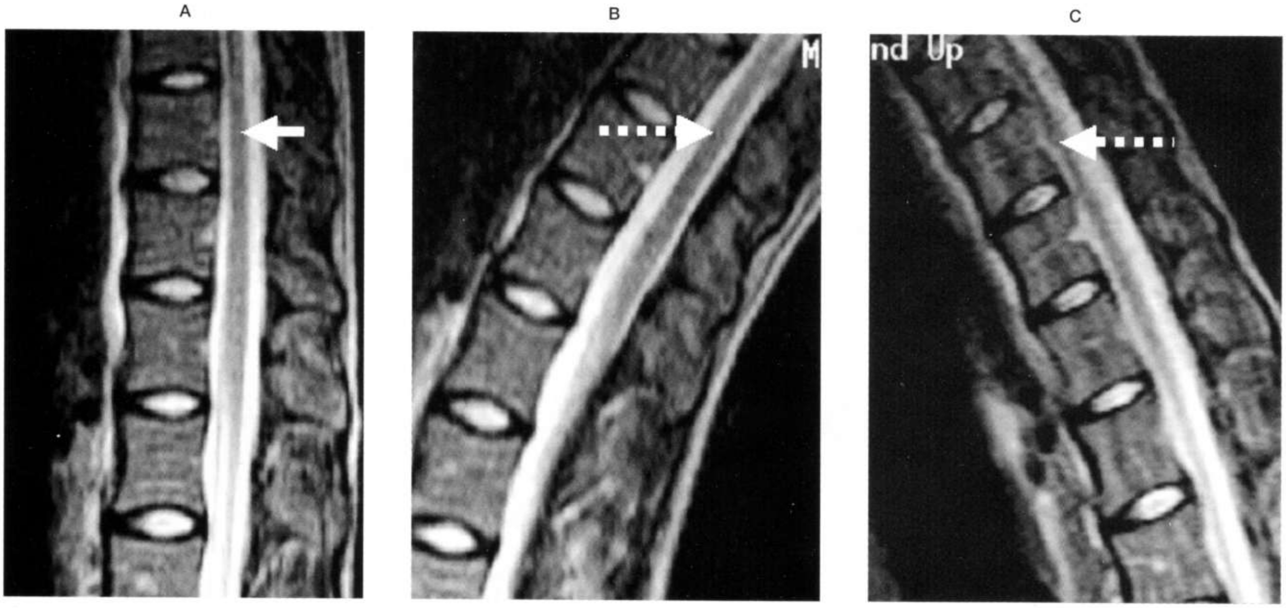

Figure 12 Spinal cord mobility analysis. A) Recumbent midline sagittal T2-weighted spin echo MRI (rMRI) shows the normal position of the conus medullaris (arrow). B) Upright-extension midline sagittal T2-weighted spin echo MRI (kMRI) demonstrates posterior movement of the conus medullaris within the spinal subarachnoid space (dashed arrow). C) Upright-flexion midline sagittal T2-weighted spin echo MRI (kMRI) reveals anterior displacement of the spinal cord (dashed arrow). This study shows normal distal spinal cord mobility. This type of evaluation may enable the analysis of clinically suspected cases of congenital or postoperative spinal cord tethering.

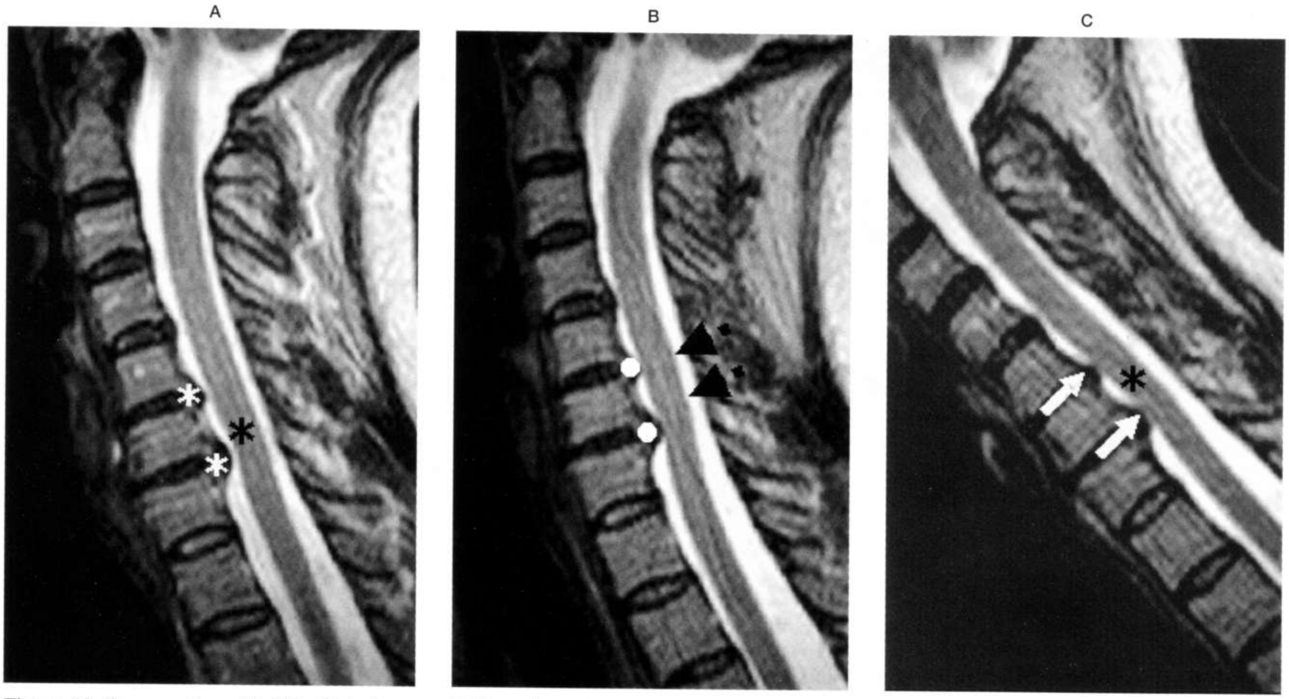

Figure 13 Provocative p/kMRI: clinical case of "Lhermitte's Syndrome", or electrical sensations extending down both upper extremities upon flexion of the cervical spine. A) Recumbent midline sagittal T2-weighted spin echo MRI (rMRI) shows the normal appearance of the cervical spinal cord (black asterisk) and the two level posterior disc protrusions at the C5-C6 and C6-C7 levels (white asterisks). B) Upright-neutral midline sagittal T2-weighted spin echo MRI (kMRI) demonstrates anterior displacement of the spinal cord (dashed arrows), now resting against the posterior disc protrusions (dots). C) Upright-flexion midline sagittal T2-weighted spin echo MRI (kMRI) reveals draping of the spinal cord (asterisk) over the two posterior disc protrusions (arrows). The patient only manifested symptoms consistent with Lhermitte's Syndrome during this flexion study. This study shows the potential provocative nature of dynamic-kinetic MRI (kMRI) in its ability to correlate a specific imaging acquisition with a specific clinical syndrome.

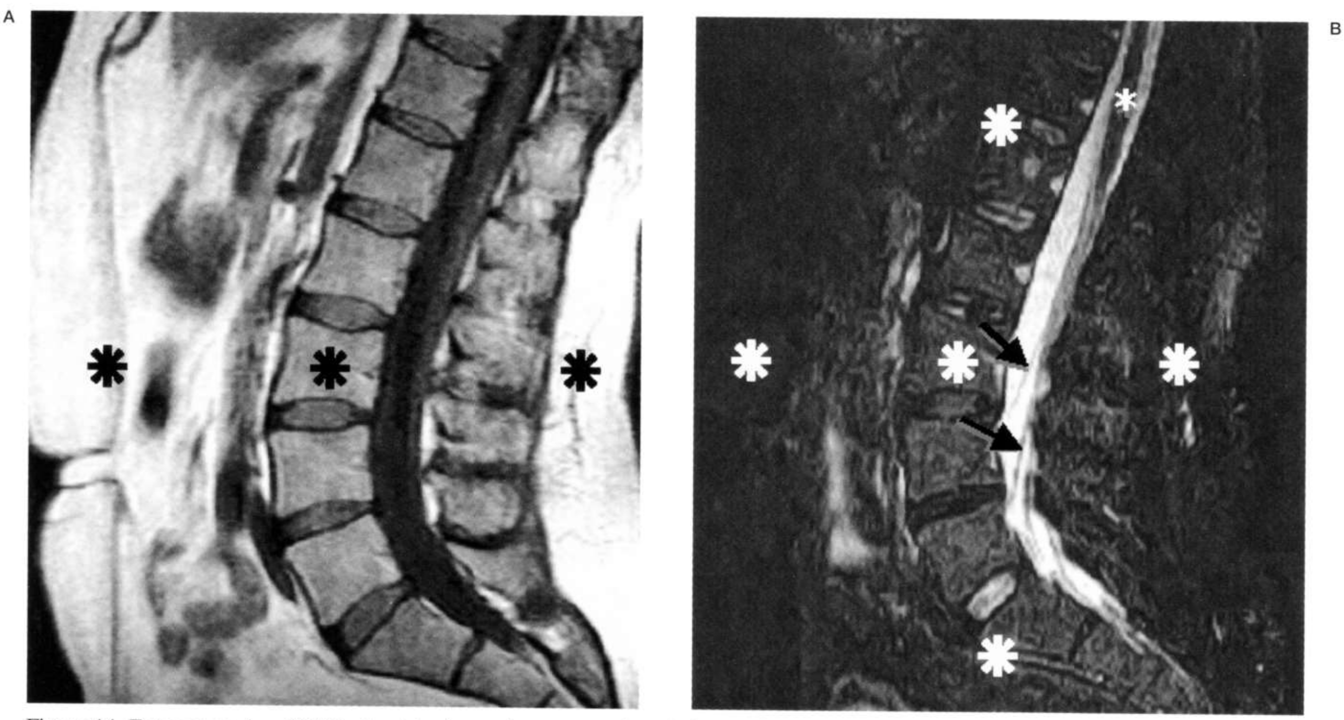

Figure 14 Fat suppression (STIR: short tau inversion recovery) technique. A) Recumbent midline sagittal T1-weighted fast spin echo MRI (rMRI) shows normal vertebral marrow, epidural and perivertebral fat (asterisks). B) Recumbent midline sagittal T2-weighted fast spin echo MRI (rMRI) with fat suppression (STIR) shows excellent fat suppression equally across the entire image (large asterisks). Note the good visualization of the conus medularis (small asterisk) and the nerve roots of the cauda equina (arrows).

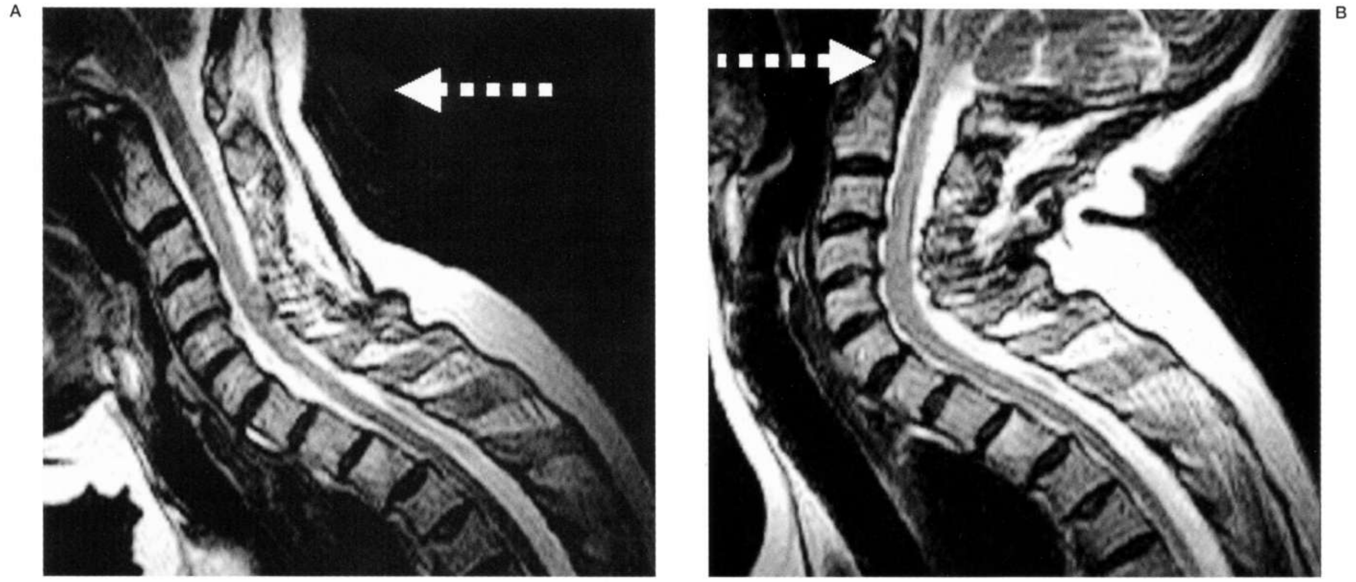

Figure 15 Ultra-fast imaging techniques for application with spinal stress maneuvers: kMRI. A) Upright-flexion (arrow) midline sagittal T2-weighted driven-equilibrium MRI (kMRI) demonstrates normal spinal column mobility. B) Upright-extension (arrow) midline sagittal T2-weighted driven-equilibrium MRI (kMRI) again shows normal spinal column mobility. Note that there is some increase in the posterior disc protrusions at multiple levels, increased infolding of the posterior spinal ligamentous structures, and consonant minor, noncompressive narrowing of the anteroposterior dimension of the spinal canal. These single-slice, driven-equilibrium images were each acquired in thirty-four seconds (time: 17 sec x 2 NEX = 34 sec). This technique will likely prove to be important in cases of critical stenosis of the central spinal canal under conditions of hypermobile instability, where the spinal cord may be in danger of compression during stress maneuvers. The driven equilibrium sequences should allow very brief imaging acquisitions and enable dynamic-kinetic patient positions to be safely assumed for very short periods of time required by this technique.

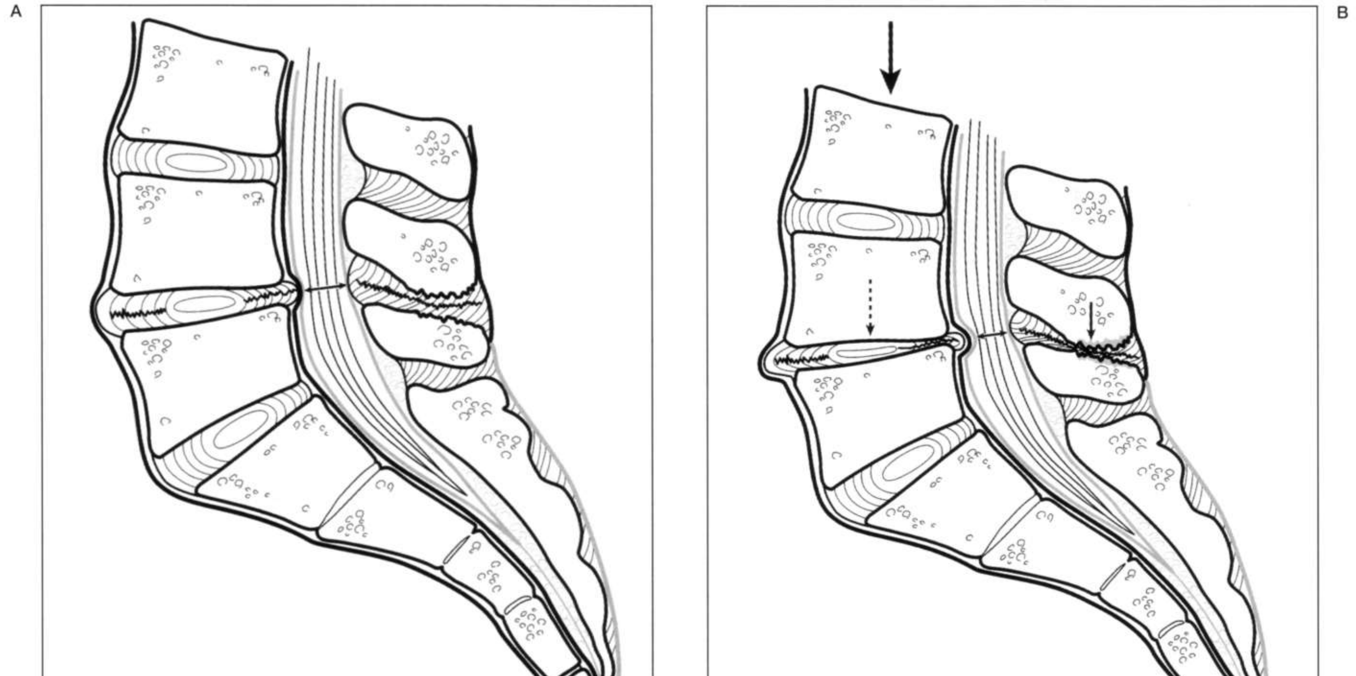

Figure 16 Telescoping of the spinal column associated with degenerative disc disease. A) Diagram of recumbent spine showing degenerative disc disease at the L4-L5 level, and degeneration of the interspinous ligament at this same level (serrated lines). Note the bulging of the degenerated intervertebral disc at L4-L5 resulting in mild narrowing of the central spinal canal (double headed arrow). B) Diagram of the upright-neutral lumbosacral spine demonstrating gravity related (large solid arrow) narrowing of the L4-L5 intervertebral disc space (dashed arrow) and interspinous space (small solid arrow) as compared to the recumbent image A, together with redundancy of the soft tissues bordering upon the central spinal canal. This telescoping of the spinal column may result in varying degrees of worsening stenosis of the central spinal canal (double headed arrow).

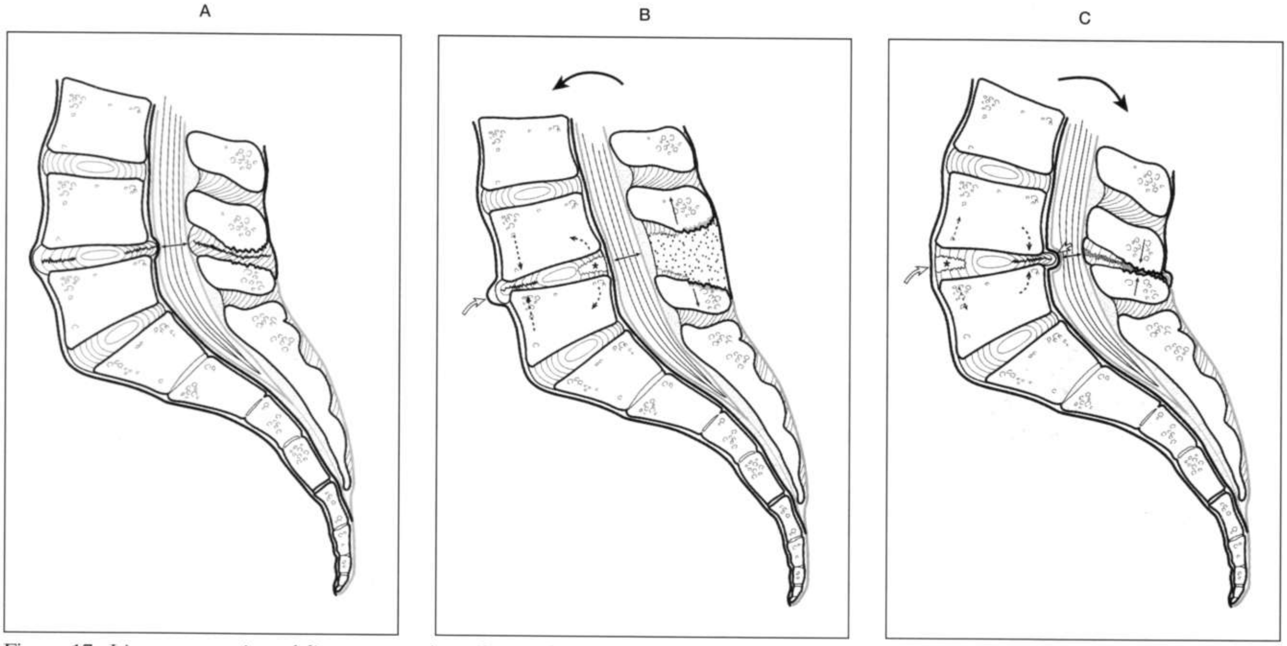

Figure 17 *Ligamentotactic* and *ligamentopathic* effects. A) Diagram of the recumbent spine showing degeneration of the L4-L5 intervertebral disc and interspinous ligament (serrated lines). Note the mild peripheral bulging of the intervertebral disc at L4-L5, and the minor narrowing of the central spinal canal (double headed arrow). Also note the near parallel position of the intervertebral end plates on either side of the L4-5 disc. B) Diagram of the upright-flexed (solid curved arrow) lumbosacral spine shows an increase in the anterior disc protrusion (open curved arrow) related to laxity of the anterior longitudinal ligament and anterior fibers of the annulus fibrosus, lessening of the posterior disc protrusion/bulge caused by tension of the posterior longitudinal ligament and remaining intact posterior fibers of the annulus fibrosus, splaying of the spinous processes (solid straight arrows), hyperexpansion of the interspinous space (stippling), opening up of the posterior aspect of the disc space (asterisk, dashed curved arrows), and narrowing of the anterior aspect of the disc space (straight dashed arrows). Note that the central spinal canal becomes wider (double headed arrow) as compared to the neutral position or extension maneuver (A,C). Also note that the opposed vertebral endplates on either side of the degenerated L4-5 intervertebral disc assume an anteriorly directed wedge configuration (dysfunctional intersegmental motion: C). C) Diagram of the upright-extended lumbosacral spine shows an increase in the posterior disc protrusion (open straight arrow) related to laxity of the posterior longitudinal ligament and anterior fibers of the annulus fibrosus, lessening of the anterior disc protrusion caused by tension of the anterior longitudinal ligament and remaining intact anterior fibers of the annulus fibrosus, collision of the spinous processes (solid straight arrows), opening up of the anterior disc space (asterisk, dashed straight arrows), and narrowing of the posterior aspect of the disc space (dashed curved arrows). Note that the central spinal canal becomes narrower (double headed arrow) as compared to the neutral position or flexion maneuver (A,B). Also note that the opposed vertebral endplates on either side of the degenerated L4-5 intervertebral disc assume a posteriorly directed wedge configuration. This latter observation indicates dysfunctional intersegmental motion at this level of disc degeneration, a result in part of intersegmental ligamentopathy (i.e., ligamentous laxity/rupture).

The postoperative spine may perhaps be best analyzed by p/kMRI in those patients who have undergone surgical intersegmental fusion procedures [69]. In the absence of ferromagnetic fusion implants, the MRI unit was capable of identical evaluation as compared to the preoperative spine. Cases of stabile intersegmental fusion, for example, showed no evidence of intersegmental motion, thereby confirming postoperative intersegmental stability (figure 8). Overall mobility of the spine may also be negatively impacted by discectomy alone, unaccompanied by surgical bony fusion [70].

Spinal cord motion is another dynamic factor that may be amenable to analysis in cases where there is clinically suspected congenital or postoperative spinal cord *tethering*. In test cases, for example, the conus medullaris was seen to freely move anteriorly and posteriorly on flexion and extension kMRI, respectively (figure 10).

Provocative p/kMRI is an experimental technique that may be of major practical relevance in the future. By comparing images where the patient is pain or symptom free, with a specific position in which the patient experiences pain or symptom(s), the imaging specialist may be able to clearly link the medical images with the clinical syndrome. In this manner, provocative p/kMRI may become a truly *specific* diagnostic imaging method in cases of spinal disease (figure 11).

The images of the cervical and lumbar spine suffered very little from motion artifacts from either CSF or body origin; no study was degraded to the point of being uninterpretable. Patient motion was not a problem, this being overcome by simply placing the scan table at 5 degrees posterior tilt enabling the patient to passively rest against the table during the MRI acquisitions. In addition, it

A

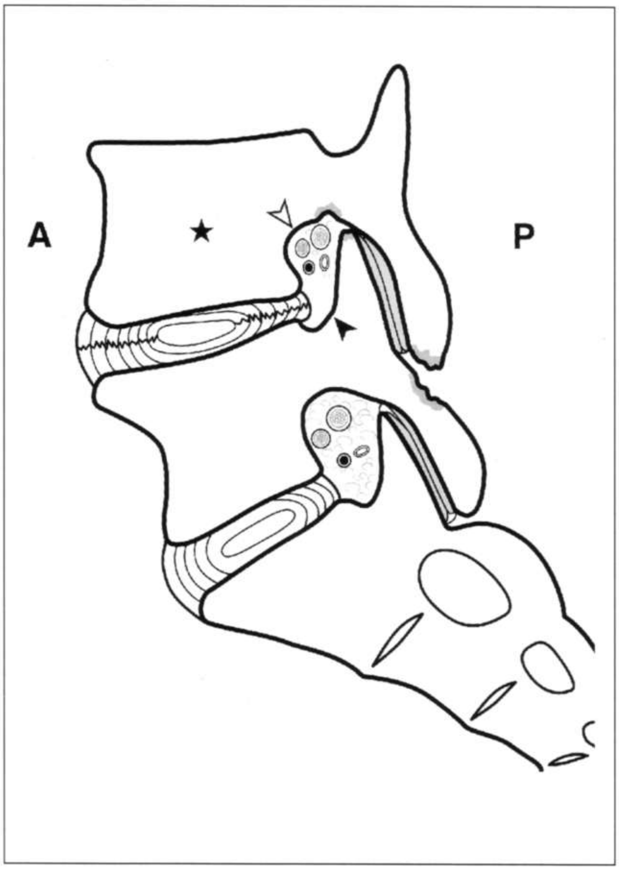

B

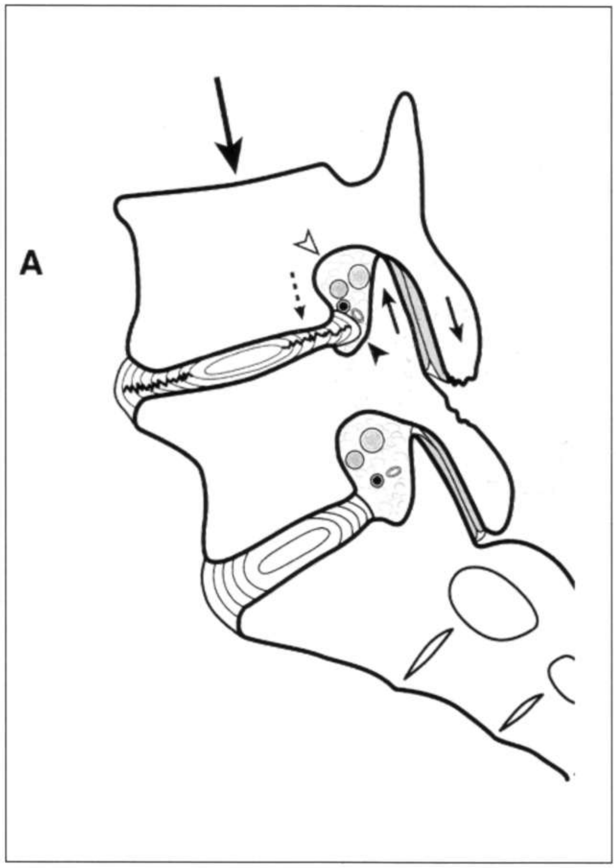

Figure 18 Effects of weight bearing-neutral posture (upright-neutral gravity and muscular balance effects), and dynamic-kinetic maneuvers on the neural foramina; dysfunctional intersegmental motion (DIM) at levels of disc degeneration. A) Diagram of the recumbent spine showing degeneration of the L4-L5 intervertebral disc (serrated lines). Note the minor narrowing of the neural foramen at this level (open arrowhead). The inferior recess of the neural foramen remains open (solid arrowhead). Also note the near parallel position of the intervertebral end plates on either side of the L4-L5 disc. B) Diagram of the upright-neutral spine (large solid straight arrow: standing postural axial loading) showing degeneration of the L4-L5 intervertebral disc (serrated lines). Note the minor increase in narrowing of the neural foramen at this level (open arrowhead: compare with A). The inferior recess of the neural foramen is further narrowed (solid arrowhead) by the increasing protrusion of the posterolateral aspect of the intervertebral disc (dashed arrow: compare with A). Also note the minor reduction in superoinferior height of the bony margins of the neural foramen, in part as a result of the disc space narrowing (dashed arrow) associated with subluxation of the spinal facet joint articular processes (small straight solid arrows).

was found to be unnecessary to stand the patient for upright p/kMRI of the cervical and thoracic spines; at present, only one sagittal sequence is felt to be necessary for evaluation of the lumbar spine, in order to analyze the lumbosacral spine for true postural curvature and for considering issues of *spinal balance* [71-74].

The remainder of the lumbosacral spine p/k MRI examination may be performed in the sitting position.

The chemical shift artifact was minor on all images, this being directly related to field strength; this effect would be expected to be less than one-half that experienced at 1.5 T. In addition, the degree of motion artifact from such sources as the heart or CSF motion was typically minor, even without 'flow compensation'overlay techniques that were not used; this source of artifacts is also related to field strength, commonly being worse on high-field MRI units.

Other currently relevant overlay techniques are possible on this p/kMRI unit. Included among these are fat suppression imaging (STIR: short tau inversion recovery) coupled with fast spin echo acquisitions (figure 12). This is felt to be very useful in the evaluation of spinal inflammation and spinal neoplasia.

Finally, in the patient with a possible critical stenosis of the spine in association with hypermobile instability or positional worsening of the narrowing of the central spinal canal, long time period acquisition sequences are of concern in the patient who may have greater degrees of spinal cord or cauda equina compression in upright flexion-ex-

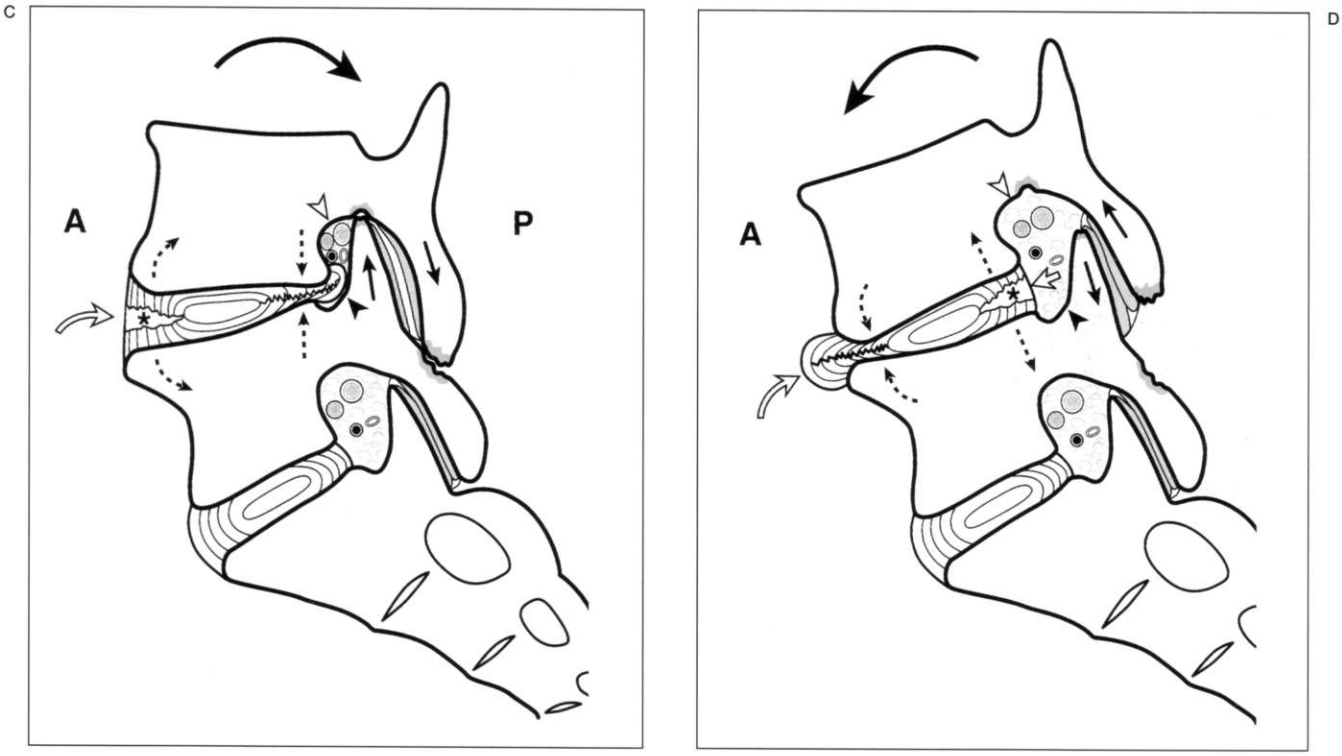

Figure 18 C) Diagram of the upright-extended (curved solid arrow) lumbosacral spine shows, an increase in the posterior disc protrusion/bulge, and narrowing of the posterior aspect of the disc space (straight dashed arrows). Note the increasing posterior disc protrusion associated with obliteration of the inferior recess (solid arrowhead) and superior recess (open arrowhead) of the neural foramen (solid arrowhead), the opening up of the anterior disc space (asterisk, dashed curved arrows), the narrowing of the posterior aspect of the disc space (straight dashed arrows), the partial shearing contracting subluxation of the posterior spinal facet (zygapophyseal) joint processes (solid straight arrows), and the diminution in size of the anteriorly bulging disc (open curved arrow). Also note that the opposed vertebral endplates on either side of the degenerated L4-5 intervertebral disc assume a posteriorly directed wedge configuration (dysfunctional intersegmental motion: C). D) Diagram of the upright-flexed (solid curved arrow) lumbosacral spine demonstrating anterior disc protrusion (open curved arrow) related to laxity of the anterior longitudinal ligament, lessening of the posterior disc protrusion/bulge as a result of tension of the remaining intact posterior annular fibers, opening up of the posterior aspect of the disc space (asterisk, straight dashed arrows), narrowing of the anterior aspect of the disc space (curved dashed arrows), the partial shearing distracting subluxation of the posterior spinal facet (zygapophyseal) joint processes (solid straight arrows), and the opening up of the superior recess (solid arrowhead) and inferior recess (open arrowhead) of the spinal neural foramen. Also note that the opposed vertebral endplates on either side of the degenerated L4-5 intervertebral disc assume an anteriorly directed wedge configuration. This latter observation indicates dysfunctional intersegmental motion at this level of disc degeneration, a result in part of intersegmental ligamentopathy (i.e., ligamentous laxity/rupture).

tension p/kMRI. For this purpose, very fast acquisition sequences have been implemented in order to screen for such critical abnormalities before going forward with longer time period imaging studies (e.g., ~4-5 minutes). Driven-equilibrium fast spin echo acquisitions offer excellent quality imaging in a fraction of the time (e.g., 1 NEX = 17 seconds) required of traditional sequences, and allow safe imaging of almost any patient with p/kMRI (figure 13). These fast high-resolution techniques may in the future be a major if not only method of imaging the spine using p/kMRI.

Conclusions

To conclude, the potential relative beneficial aspects of upright, weight-bearing (pMRI), dynamic-kinetic (kMRI) spinal imaging on this system over that of recumbent MRI (rMRI) include: clarification of true sagittal upright neutral spinal curvature unaffected by patient positioning, revelation of occult degenerative spinal disease dependent on true axial loading (i.e., weight-bearing) (figure 14), unmasking of kinetic-dependent degenerative spinal disease (i.e., flexion-extension) (figures 15-17), and the potential ability to scan the patient in the position of clinically relevant pain (figure 11) (table 9). Scanning the patient in the *operative position*, enabling the surgeon to have a true preoperative picture of the intraoperative pathologic morphology, is a topic currently under investigation [75]. This MRI unit also demonstrated low claustrophobic potential and yielded high-resolution images with little motion/chemical artifact.

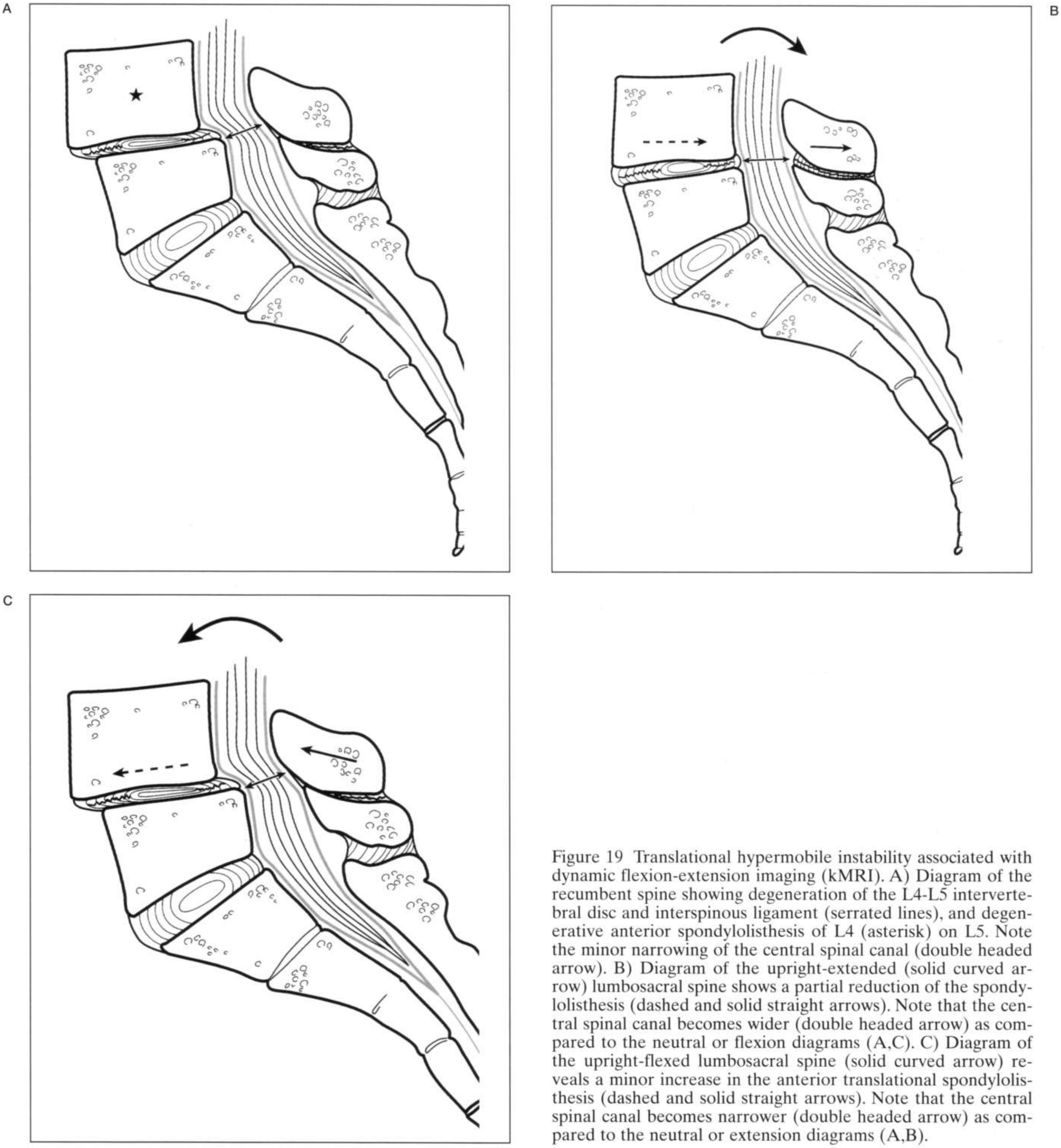

Figure 19 Translational hypermobile instability associated with dynamic flexion-extension imaging (kMRI). A) Diagram of the recumbent spine showing degeneration of the L4-L5 intervertebral disc and interspinous ligament (serrated lines), and degenerative anterior spondylolisthesis of L4 (asterisk) on L5. Note the minor narrowing of the central spinal canal (double headed arrow). B) Diagram of the upright-extended (solid curved arrow) lumbosacral spine shows a partial reduction of the spondylolisthesis (dashed and solid straight arrows). Note that the central spinal canal becomes wider (double headed arrow) as compared to the neutral or flexion diagrams (A,C). C) Diagram of the upright-flexed lumbosacral spine (solid curved arrow) reveals a minor increase in the anterior translational spondylolisthesis (dashed and solid straight arrows). Note that the central spinal canal becomes narrower (double headed arrow) as compared to the neutral or extension diagrams (A,B).

Based on initial experience with this unit, it is felt that mid-field MRI may prove to be the optimal field strength for routine, anatomic MR imaging of the spinal column in degenerative as well as other spinal disease categories[76].

In addition, the evidence thus far indicates that p/kMRI may prove to be efficacious to incorporate as a part of the diagnosis-treatment paradigm in patients with spinal, radicular and referred pain syndromes originating from spinal pathology (table 10).

References

1 Jinkins JR: Atlas of Neuroradiologic Embryology, Anatomy and Variants. Lippincott-Williams and Wilkins (ed), Philadelphia 2000.
2 Jinkins JR, Green C, Damadian R: Upright, Weight-Bearing, Dynamic-Kinetic MRI of the Spine: pMRI/kMRI. Rivista di Neuroradiologia 14: 135, 2001.
3 Smith TJ, Fernie GR: Functional Biomechanics of the Spine. Spine 16: 1197-1203, 1991.
4 Smith TJ: In Vitro Spinal Biomechanics: Experimental Methods and Apparatus. Spine 16: 1204-1210, 1991.
5 Marras WS, Granata KP: A Biomechanical Assessment and Model of Axial Twisting in the Thoracolumbar Spine. Spine 20: 1440-1451, 1995.
6 Resnick DK, Weller SJ, Benzel EC: Biomechanics of the Thoracolumbar Spine. Neurosurg Clin N Amer 8: 455-469, 1997.
7 Berne D, Goubier JN et Al: The Aging of the Spine. Eur J Orthop Surg Traumatol 9: 125-133, 1999.
8 Boden SD, Wiesel SW: Lumbosacral Segmental Motion in Normal Individuals: Have We Been Measuring Instability Properly? Spine 15: 571-576, 1990.
9 Danielson BI, Willén J et Al: Axial Loading of the Spine During CT and MR in Patients with Suspected Lumbar Spinal Stenosis. Acta Radiol 39: 604-611, 1998.
10 Frymoyer JW, Frymoyer WW et Al: The Mechanical and Kinematic Analysis of the Lumbar Spine in Normal Living Human Subjects in Vivo. J Biomech 12: 165-172, 1979.
11 Hedman TP, Fernie GR: In Vivo Measurement of Lumbar Spinal Creep in Two Seated Postures Using Magnetic Resonance Imaging. Spine 20: 178-183, 1995.
12 Hilton RC, Ball J, Benn RT: In-vitro mobility of the lumbar spine. Annals Rheum Dis 38: 378-383, 1979.
13 Inufusa A, An HS et Al: Anatomic Changes of the Spinal Canal and Intervertebral Foramen Associated With Flexion-Extension Movement. Spine 21: 2412-2420, 1996.
14 Mayoux-Benhamou MA, Revel M et Al: A Morphometric Study of the Lumbar Foramen: Influence of Flexion-Extension Movements and of Isolated Disc Collapse. Surg Radiol Anat 11: 97-102, 1989.
15 Nachemson AL, Schultz AB, Berkson MH: Mechanical Properties of Human Lumbar Spine Motion Segments: Influences of Age, Sex, Disc Level, and Degeneration. Spine 4: 1-8, 1979.
16 Nowicki BH, Haughton VM et Al: Occult Lumbar Lateral Spinal Stenosis in Neural Foramina Subjected to Physiologic Loading. Am J Neuroradiol 17: 1605-1614, 1996.
17 Pennal GF, Conn GS et Al: Motion Studies of the Lumbar Spine: A Preliminary Report. J Bone Joint Surg 54B: 442-452, 1972.
18 Penning L, Wilmink JT: Posture-dependent Bilateral Compression of L4 or L5 Nerve Roots in Facet Hypertrophy: A Dynamic CT-Myelographic Study. Spine 12: 488-500, 1987.
19 Schönström N, Lindahl S et Al: Dynamic Changes in the Dimensions of the Lumbar Spinal Canal: An Experimental Study In Vitro. J Orthop Res 7: 115-121, 1989.
20 Sortland O, Magnes B, Hauge T: Functional Myelography With Metrizamide in the Diagnosis of Lumbar Spinal Stenosis. Acta Radio 355 (suppl): 42-54, 1977.
21 White AS, Panjabi MM: The Basic Kinematics of the Human Spine: A Review of Past and Current Knowledge. Spine 3: 12-29, 1978.
22 Willén J, Danielson B et Al: Dynamic Effects on the Lumbar Spinal Canal: Axially Loaded CT-Myelography and MRI in Patients with Sciatica and/or Neurogenic Claudication. Spine 22: 2968-2976, 1997.
23 Wilmink JT, Penning L, van den Burg W: Role of stenosis of spinal canal in L4-L5 nerve root compression assessed by flexion-extension myelography. Neuroradiology 26: 173-181, 1984.
24 Friberg O: Lumbar Instability: A Dynamic Approach by Traction, Compression Radiography. Spine 12: 119-120, 1987.
25 Fujiwara A, An HS et Al: Morphologic Changes in the Lumbar Intervertebral Foramen Due to Flexion-Extension, Lateral Bending, and Axial Rotation: An In Vitro Anatomic and Biomechanical Study. Spine 26: 876-882, 2001.
26 Hayes MA, Howard TC et Al: Roentgenographic Evaluation of Lumbar Spine Flexion-Extension in Asymptomatic Individuals. Spine 14: 327-331, 1989.
27 Lee RR, Abraham RA, Quinn CB: Dynamic Physiologic Changes in Lumbar CSF Volume Quantitatively Measured By Three-Dimensional Fast Spin-Echo MRI. Spine 26: 1172-1178, 2001.
28 Panjabi MM, Takata K, Goel VK: Kinematics of Lumbar Intervertebral Foramen. Spine 8: 348-357, 1983.
29 Pearcy MJ, Tibrewal SB: Axial Rotation and Lateral Bending in the Normal Lumbar Spine Measured by Three-Dimensional Radiography. Spine 9: 582-587, 1984.
30 Penning L, Wilmink JT: Biomechanics of Lumbosacral Dural Sac. A Study of Flexion-Extension Myelography. Spine 6: 398-408, 1981.
31 Revel M, Mayoux-Benhamou MA et Al: Morphological variations of the lumbar foramina. Rev Rhum Mal Osteoartic 55: 361-366, 1988.
32 Stokes IA, Frymoyer JW: Segmental Motion and Instability. Spine 12: 688-691, 1987.
33 Stokes IA, Wilder DG et Al: Assessment of Patients with Low-Back Pain by Biplanar Radiographic Measurement of Intervertebral Motion. Spine 6: 233-240, 1981.
34 Takayanagi K, Takahashi K et Al: Using Cineradiography for Continuous Dynamic-Motion Analysis of the Lumbar Spine. Spine 26: 1858-1865, 2001.
35 Wildermuth S, Zanetti M et Al: Lumbar Spine: Quantitative and Qualitative Assessment of Positional (Upright Flexion and Extension) MR Imaging and Myelography. Radiology 207: 391-398, 1998.
36 Wisleder D, Smith MB et Al: Lumbar Spine Mechanical Response to Axial Compression Load In Vivo. Spine 26: E403-409, 2001.
37 Wisleder D, Werner SL et Al: A Method to Study Lumbar Spine Response to Axial Compression During Magnetic Resonance Imaging. Spine 26: E416-E420, 2001.
38 Zamani AA, Moriarty T et Al: Functional MRI of the Lumbar Spine in Erect Position in a Superconducting Open-Configuration MR System: Preliminary Results. JMRI 8: 1329-1333, 1998.
39 Leviseth G, Drerup B: Spinal shrinkage during work in a sitting posture compared to work in a standing posture. Clin Biomech 12: 409-418, 1997.
40 Lowe, RW, Hayes TD et Al: Standing Roentgenograms in Spondylolisthesis. Clin Orthop 117: 80-84, 1976.
41 Devor M, Rappaport ZH: Relation of Foraminal (Lateral) Stenosis to Radicular Pain. Am J Neuroradiol 17: 1615-1617, 1996.
42 Hasegawa T, An HS et Al: Lumbar Foraminal Stenosis: Critical Heights of the Intervertebral Discs and Foramina. J Bone Joint Surg 77-A: 32-38, 1995.
43 Pfirrmann CWA, Metzdorf A, Zanetti M: Magnetic Resonance Classification of Lumbar Intervertebral Disc Degeneration. Spine 26: 1873-1878, 2001.
44 Shiwei Y, Haughton VM, Sether LA: Criteria for Classifying Normal and Degenerated Lumbar Intervertebral Disks. Neuroradiology 170: 523-526, 1989.
45 Axelsson P, Johnson R, Strömqvist B: Is There Increased Intervertebral Mobility in Isthmic Adult Spondylolisthesis? A Matched Comparative Study Using Roentgen Stereophotogrammetry. Spine 25: 1701-1703, 2000.
46 Boden SD, Frymoyer JW: Segmental Instability: Overview and Classification. In: Frymoyer JW (ed): The Adult Spine: Principles and Practice. Lippincott-Raven, Philadelphia 1997: 2137-2155.
47 Dupuis PR, Yong-Hing K et Al: Radiologic Diagnosis of Degenerative Lumbar Spinal Instability. Spine 10: 262-276, 1985.
48 Frymoyer JW, Selby DK: Segmental Instability: Rationale for Treatment. Spine 10: 280-286, 1985.
49 Fujiwara A, Lim T-H et Al: The Effect of Disc Degeneration and Facet Joint Osteoarthritis on the Segmental Flexibility of the Lumbar Spine. Spine 25: 3036-3044, 2000.

50 Pearcy M, Shepherd J: Is There Instability in Spondylolisthesis? Spine 10: 175-177, 1985.
51 Ito M, Tadano S, Kaneda K: A Biomechanical Definition of Spinal Segmental Instability Taking Personal and Disc Level Differences Into Account. Spine 18: 2295-2304, 1993.
52 Pope MH, Panjabi M: Biomechanical Definitions of Spinal Instability. Spine 10: 255-256, 1985.
53 Sato H, Kikuchi S: The Natural History of Radiographic Instability of the Lumbar Spine. Spine 18: 2075-2079, 1993.
54 Posner I, White AA et Al: A Biomechanical Analysis of the Clinical Stability of the Lumbar and Lumbosacral Spine. Spine 7: 374-389, 1982.
55 Wood KB, Popp CA et Al: Radiographic Evaluation of Instability in Spondylolisthesis. Spine 7: 1697-1703, 1994.
56 Yahia H, Drouin G et Al: Degeneration of the Human Lumbar Spine Ligaments. An Ultrastructural Study. Path Res Pract 184: 369-375, 1989.
57 Fujiwara A, Tamai K et Al: The Interspinous Ligament of the Lumbar Spine: Magnetic Resonance Images and Their Clinical Significance. Spine 25: 358-363, 2000.
58 Adams MA, Hutton WC, Stott JRR: The Resistance to Flexion of the Lumbar Intervertebral Joint. Spine 5: 245-253, 1980.
59 Dumas GA, Beaudoin L, Drouin G: In Situ Mechanical Behavior of Posterior Spinal Ligaments in the Lumbar Region. An In Vitro Study. J Biomechanics 20: 301-310, 1987.
60 Hukins DWL, Kirby MC et Al: Comparison of Structure, Mechanical Properties, and Functions of Lumbar Spinal Ligaments. Spine 15: 787-795, 1990.
61 Panjabi MM: The Stabilizing System of the Spine. Part 1. Function, Dysfunction, Adaptation, and Enhancement. J Spinal Disorders 5: 383-389, 1992.
62 Panjabi MM, Goel VK, Takata K: Physiologic Strains in the Lumbar Spinal Ligaments: An In Vitro Biomechanical S-tudy. Spine 7: 192-203, 1982.
63 Sharma M, Langrana NA, Rodriguez J: Role of Ligaments and Facets in Lumbar Spinal Stability. Spine 20: 887-900, 1995.
64 Fujiwara A, Lim TH, An HS: The Effect of Disc Degeneration and Facet Joint Osteoarthritis on the Segemental Flexibility of the Lumbar Spine. Spine 25: 3036-3044, 2000.
65 Haughton VM, Schmidt TA et Al: Flexibility of Lumbar Spinal Motion Segments Correlated to Type of Tears in the Annulus Fibrosis. J Neurosurg 92: 81-86, 2000.
66 Thompson RE, Pearcy MJ et Al: Disc Lesions and the Mechanics of the Intervertebral Joint Complex. Spine 25: 3026-3035, 2000.
67 Twomey LT, Taylor JR: Sagittal Movements of the Human Lumbar Vertebral Column: A Quantitative Study of the Role of the Posterior Vertebral Elements. Arch Phys Med Rehabil 64: 322-325, 1983.
68 Cartolari R, Argento G et Al: Axial Loaded Computed Tomography (AL-CT) and Cine AL-CT. Rivista di Neuroradiologia 11, 1998.
69 Jinkins JR: Posttherapeutic Neurodiagnostic Imaging. Jinkins JR (ed), Lippincott-Raven, Philadelphia 1997.
70 Keller TS, Hansson TH et Al: In Vivo Creep Behavior of the Normal and Degenerated Porcine Intervertebral Disk: A Preliminary Report. J Spinal Disorders 1: 267-278, 1989.
71 Jackson RP, Hales C: Congruent Spinopelvic Alignment on Standing Lateral Radiographs of Adult Volunteers. Spine 25: 2808-2815, 2000.
72 Lee C-S, Lee C-K et Al: Dynamic Sagittal Imbalance of the Spine in Degenerative Flat Back. Spine 26: 2029-2035, 2001.
73 Jackson RP, Kanemura T et Al: Lumbopelvic Lordosis and Pelvic Balance on Repeated Standing Lateral Radiographs of Adult Volunteers and Untreated Patients with Constant Low Back Pain. Spine 25: 575-586, 2000.
74 Jackson RP, Peterson MD et Al: Compensatory Spinopelvic Balance Over the Hip Axis and Better Reliability in Measuring Lordosis to the Pelvic Radius on Standing Lateral Radiographs of Adult Volunteers and Patients. Spine 23: 1750-1767, 1998.
75 Stephens GC, Yoo JU, Wilbur G: Comparison of Lumbar Sagittal Alignment Produced by Different Operative Positions. Spine 21: 1802-1807, 1996.
76 Jinkins JR: Acquired Degenerative Changes of the Intervertebral Segments at and Suprajacent to the Lumbosacral Junction: a Radioanatomic Analysis of the Nondiskal Structures of the Spinal Column and Perispinal Soft Tissues. Radiol Clin Nor Am 39: 73-99, 2001.

J. Randy Jinkins MD, FACR, FEC
Director of Craniospinal Anatomic Imaging Research
Department of Radiological Sciences
Medical College of Philadelphia-Hahnemann
Drexel University
245 North 15th Street - Mailstop 206
Philadelphia, PA 19102-1192
E-mail: jrjinkins@aol.com